CHAPTER 2

HYDRODYNAMICS AND MIXING IN ESTUARIES AND COASTAL WATERS

The main factors governing the dispersion of any substance in a waterbody are related to the existing hydrodynamic conditions. Strictly speaking, this is not true at short distances from the source in the case of effluent discharges, since the effects of the initial momentum and buoyancy of the discharge have not yet vanished. When the initial discharge effects become small enough, it is the wind, the waves, the tides and the ambient turbulence which will determine how the discharged substance is transported. A good knowledge of the hydrodynamics of the coastal waters is therefore an important issue when deciding where to build a marine outfall, or when trying to assess the effects of an accidental spill on the marine ecosystem or the nearby coast.

This chapter presents, in its first part, a review of the physical equations that govern the dynamics of fluids for laminar and turbulent flows; in the second part, an extensive description of coastal and estuarine hydrodynamics is presented, including oscillatory motion, nearshore currents, tidal currents, turbulence and estuarine circulation. The third part introduces the concept of mixing in coastal waters, and how it is related to the local hydrodynamic conditions.

2.1 CONSERVATION EQUATIONS

The behaviour of natural flow and mass transport is governed by a set of general differential equations that must be fulfilled at all points. The four equations that describe non-steady laminar flows are presented below, and form a closed system with four dependent variables that can be solved, given appropriate boundary and initial conditions. For the case of turbulent flows, as it will be seen,

the number of equations is smaller than the number of unknown variables, and turbulence models must be introduced to close the system.

2.1.1 Laminar flows

2.1.1.1 Continuity equation

The continuity equation describes the principle of conservation of mass, assuming that both velocity and mass are continuous functions of space and time. For a fixed elementary control volume of fluid, the mass conservation demands that the net mass flux entering the volume is balanced by a local change in density, i.e.,

$$\frac{\partial \rho}{\partial t} + u_j \frac{\partial \rho}{\partial x_j} + \rho \frac{\partial u_i}{\partial x_i} = 0 \tag{2.1}$$

where u_i are velocity components, x_i (and x_j) are spatial coordinates (with i, j=1, 2, 3) and ρ is the density of the fluid. If ρ is constant, i.e., the fluid is incompressible, the conservation of mass can be reduced to the conservation of volume

$$\frac{\partial u_i}{\partial x_i} = 0 \tag{2.2}$$

2.1.1.2 Navier-Stokes equation

Newton's second law applied to the previously defined control volume yields an equation for the conservation of momentum:

$$\rho \frac{\partial u_i}{\partial t} + \rho u_j \frac{\partial u_i}{\partial x_j} = \frac{\partial \sigma_{ij}}{\partial x_j} + g_i \rho \tag{2.3}$$

where σ_{ij} is a stress-tensor depending on properties of the fluid, which represents forces applied at the surface of the volume, and g_i are volume forces (usually the gravity). In this equation, the terms on the left represent the acceleration along a streamline, whereas the right-hand terms stand for the driving forces. Equation (2.3) must be linked to the water properties through an empirical relation, which is generally taken as a linear stress-strain relationship, in the form

$$\sigma_{ij} = -p\delta_{ij} + \mu\left(\frac{\partial u_i}{\partial x_j} + \frac{\partial u_j}{\partial x_i}\right) \tag{2.4}$$

where μ is the fluid's dynamic viscosity, p is the pressure, δ_{ij} is the Kronecker delta function, and it has been assumed that the fluid is isotropic and incompressible. Substituting (2.4) in (2.3), and neglecting the variations of density with respect to its absolute value -Boussinesq's approximation-, the momentum conservation equation becomes

$$\frac{\partial u_i}{\partial t} + u_j \frac{\partial u_i}{\partial x_j} = -\frac{1}{\rho_r}\frac{\partial p}{\partial x_i} + \nu \frac{\partial^2 u_i}{\partial x_j \partial x_j} + g_i \frac{\rho_r - \rho}{\rho_r} \tag{2.5}$$

where ρ_r is a reference density and ν ($=\mu/\rho_r$) the kinematic viscosity.

2.1.1.3 Fick's first law

Fick's first law states that the transport J of a scalar quantity due to a Brownian motion is proportional, and opposed in direction, to the gradient of the transported quantity:

$$J = -\lambda_F \sum_{i=1}^{3} \frac{\partial C}{\partial x_i} \tag{2.6}$$

where λ_F is a species-dependent Fickian diffusion coefficient, and C is the specific concentration of the diffusing substance.

2.1.1.4 Equation of state

The equation of state links the density of the fluid to its content of heat, salt and dissolved substances. In a general form it is written as

$$\rho = f(T,S) \tag{2.7}$$

where T is the temperature and S the salinity. The exact form of equation (2.7) must be determined either mathematically or empirically (e.g., Fischer *et al.*, 1979; Wood *et al.*, 1993).

2.1.1.5 Transport equation

The equation that describes the transport of a substance in a laminar flow can be obtained combining Fick's first law and the conservation of mass for an elementary volume of fluid, and is

$$\frac{\partial C}{\partial t} + u_j \frac{\partial C}{\partial x_j} = \lambda_F \frac{\partial^2 C}{\partial x_j \partial x_j} \tag{2.8}$$

2.1.2 Turbulent flows. The closure problem

Due to the presence of turbulent motion in most flows, the relevant dependent variables appear as a complicated pattern of random fluctuations; therefore, a description of the flow at all points in time and space by means of the instantaneous continuity and momentum equations (2.1) and (2.5) is no longer possible. Instead, in order to reduce the amount of information, new equations which govern only mean quantities of the flow are developed. The usual approach is to take the mean quantities to be time-averages, defined as

$$\overline{F} = \frac{1}{t_{12}} \int_{t_1}^{t_2} F dt \tag{2.9}$$

where F is any variable, and the averaging time $t_{12} = t_2 - t_1$ is long compared to the timescale of the turbulent fluctuations. These time-averages, denoted by an overbar, have the following properties:

$$\begin{aligned} &\overline{F} + \overline{G} = \overline{F + G} \\ &\overline{\overline{F} \bullet G} = \overline{F} \bullet \overline{G} \\ &\overline{\frac{\partial F}{\partial x}} = \frac{\partial \overline{F}}{\partial x} \\ &\overline{cF} = c\overline{F} \qquad c = \text{constant} \end{aligned} \tag{2.10}$$

All dependent variables can then be decomposed into a mean component describing the mean flow, and a fluctuating component arising from the turbulent behaviour of the instantaneous flow. Thus, the velocity, the hydrodynamic pressure and the scalar concentration can be written as

$$\begin{aligned} u_i &= \overline{u}_i + u'_i \\ p &= \overline{p} + p' \\ C &= \overline{C} + c' \end{aligned} \tag{2.11}$$

where the primed variables denote fluctuating quantities.

Substituting (2.11) into equations (2.2) to (2.8) and time-averaging yields the following form for the conservation equations in turbulent flows, bearing in mind that the mean value of a fluctuating quantity is zero.

2.1.2.1 Continuity equation

$$\frac{\partial}{\partial x_i}(\overline{u_i + u'_i}) = \frac{\partial \overline{u}_i}{\partial x_i} = 0 \tag{2.12}$$

2.1.2.2 Momentum equation

Averaging of the Navier-Stokes equation (2.5) eliminates all fluctuations from the linear terms, so that only non-linear interaction terms remain:

$$\frac{\partial \overline{u}_i}{\partial t} + \overline{u}_j \frac{\partial \overline{u}_i}{\partial x_j} = -\frac{1}{\rho_r} \frac{\partial \overline{p}}{\partial x_i} + \frac{\partial}{\partial x_j} \left(-\overline{u'_i u'_j} + \nu \frac{\partial \overline{u}_i}{\partial x_j} \right) + g_i \frac{\rho_r - \rho}{\rho_r} \tag{2.13}$$

2.1.2.3 Transport equation

$$\frac{\partial \overline{C}}{\partial t} + \overline{u}_j \frac{\partial \overline{C}}{\partial x_j} = \frac{\partial}{\partial x_j}\left(\lambda_F \frac{\partial \overline{C}}{\partial x_j} - \overline{u'_j c'} \right) + Q_{SC} \qquad (2.14)$$

The new term added on the right-hand side of the equation, Q_{SC}, includes all sources and sinks of the transported substance.

2.1.2.4 The closure problem

The three equations arising from (2.13) are also known as Reynolds equations. The new terms ($\overline{u'_i u'_j}$) introduced by the averaging process due to the non-linearity of (2.13) are called Reynolds stresses, and are the unknown correlations between fluctuating velocities; similar correlations between fluctuating velocity and scalar fluctuations appear in equation (2.14). Physically these terms, multiplied by the density, represent the transport of momentum, heat or mass by the turbulent motion. The Reynolds stresses arise only because of the time-averaging process, so at a given instant the only stresses acting on a point of the fluid are the viscous stresses.

The Reynolds equations and (2.14) can be solved for the mean values of pressure, velocity and temperature/concentration only when the nine correlations in the hydrodynamic equations and the three in the transport equation can be somehow determined. The total number of unknown correlations can be reduced by noticing that the Reynolds stress tensor τ_{ij}=-ρ $\overline{u'_i u'_j}$ is symmetric (i.e., $\tau_{ij} = \tau_{ji}$) but that still leaves a total of six unknown correlations. Additional symmetry about the vertical direction is sometimes assumed, thus reducing further the number of unknowns to two, one in the horizontal plane (τ_H) and one in the vertical direction (τ_V). Measurements of τ_H and τ_V by different researchers have given values for the latter of order 10^1 cm^2/s, and several orders of magnitude higher for the former.

The most direct approach is to try to close the system of equations (2.12) - (2.14) by deriving new expressions, describing the turbulent correlations, directly from the Navier-Stokes equations,. Exact transport equations can be found for $\overline{u'_i u'_j}$ and $\overline{u'_i c'}$ but these contain turbulent correlations of the next higher order (i.e., $\overline{u'_i u'_j u'_k}$). It can be proved that exact transport equations can be derived for any-order correlations, but higher-order correlations will always keep appearing. This fundamental problem is referred to as the “turbulence closure problem”, and makes it necessary to find other ways of closing the system (see §2.3.1.1).

2.2 COASTAL HYDRODYNAMICS

The dynamic processes that exist in the nearshore region are generated by a number of different driving agents. Under the influence of these external forces, the fluid motion of the water manifests itself as coastal currents, tides and tidal currents, internal and surface waves, storm surges, tsunamis and others (Horikawa, 1988). Even though the effects of storm surges and tsunamis can be

destructive in coastal areas, their occurrence is rather infrequent and, therefore, they shall not be treated here.

The main difference between coastal waters and deep ocean waters is the presence of two physical constraints (i.e., the sea bottom, at a relatively shallow depth, and the coastline) which somehow determine the motion of the sea water.

The nearshore zone is defined as the region extending from a landward limit associated with storm-wave phenomena (e.g., overwash), to a seaward limit beyond the point where incident waves break, but which depends on the specific context (Horikawa, 1988). Within this zone, several other regions may be distinguished, as shown in figure 2.1, taken from Horikawa (1988). The most relevant of these are, for the purposes of the following description of hydrodynamics in coastal waters, the breaker zone, the breaking point, and the surf zone. The former is the zone where incident irregular waves break; the breaking point is where breaking begins and the waves attain maximum height, and the surf zone is defined as the region between the seaward limit of the breaker zone and the area of high turbulence created by the collision of the backrushing water mass and the incoming waves (Horikawa, 1988).

Following Sánchez-Arcilla and Lemos (1990), the relevant phenomena in the surf zone can be classified into four different types:

a) Sediment transport and corresponding changes in morphology, with a characteristic time scale of 1 day to 1 month, and a spatial scale between 100 m and 1000 m.

b) Currents (non-oscillatory flow), with time scales between 10 minutes and 1 hour, and spatial scales similar to those of sediment transport.

c) Organised oscillatory flows (i.e., wind waves, infra-gravity waves), with time scales ranging from 10^{-1} sec to 10 min, and space scales from 1 to 100 m.

d) Random oscillatory flow (turbulence), whose length scales are between 10^{-3} to 10^{1} sec , and with small (10^{-4} to 10^{-1} m) spatial scales.

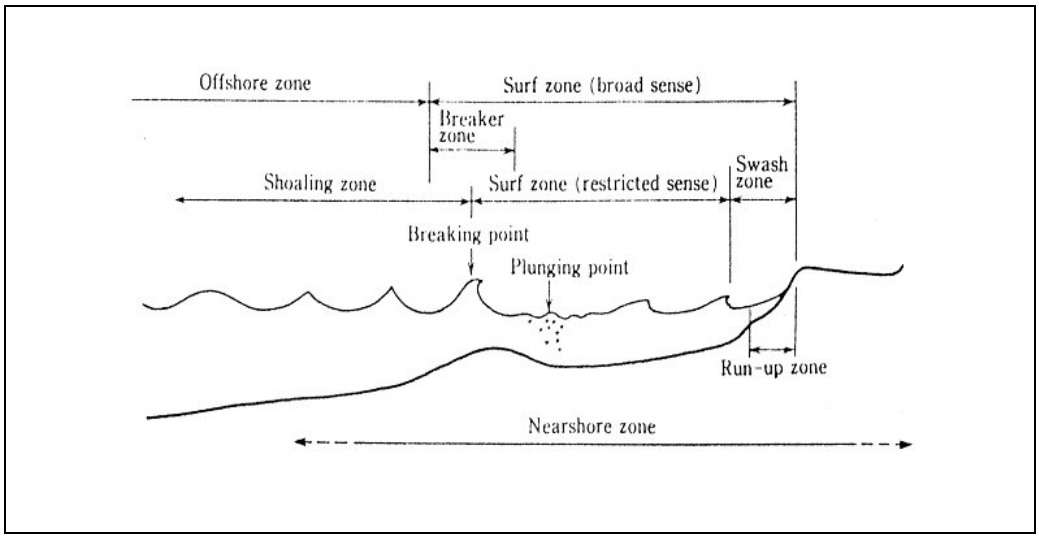

Figure 2.1: Zone division in the nearshore region (from Horikawa, 1988).

In a general overview, it can be said that the main features in coastal hydrodynamics are the wind waves, generated by the stress exerted on the ocean surface by the wind. As these waves travel from deep waters into shallower regions, they become more non-linear and dissipative, transferring energy from the peak of the spectrum to higher and lower frequencies. Eventually, the proximity of the sea bottom will induce the breaking of the waves, producing a severe increase in the marine turbulence level, and generating different types of currents, which may extend beyond the surf zone.

However, the study of nearshore hydrodynamics is not an easy task. Wave, current and turbulence scales tend to overlap, thus giving rise to the interaction (to some degree) of these three flow types; since the individual flows are non-linear in nature, their interaction becomes quite complex. The usual procedure followed to derive and understand the governing equations is to decompose all the state variables into contributions from currents, waves and turbulence, and then use time-averaging operators to isolate the desired phenomenon. This process is essentially the same as the one followed in §2.1.2 to obtain the conservation equations for general turbulent flows and, as in that case, the closure problem also arises here because of the non-linearity of the momentum equations.

2.2.1 Wind-induced currents

As the wind blows over the sea surface, it exerts a tangential stress on the upper layer of the water that will eventually generate the surface waves. To obtain the parameters which characterise the wind-induced currents, it is assumed that the controlling parameters of the wind field are:

- average wind speed U_W at some height (z) above the still water surface (usually z = 10m)
- wind fetch X_W
- wind duration t_W

The mean velocity $U_W(z)$ at a fixed height is given by

$$U_W(z) = \frac{u_*^S}{\kappa}\left[\ln\left(\frac{z}{z_0}\right) + f(Ri)\right] \tag{2.15}$$

where u^S_* is the friction or surface shear velocity, defined as

$$u_*^S = \sqrt{\frac{\tau_s}{\rho_{ar}}} \tag{2.16}$$

and τ_s is the surface stress, ρ_{ar} is the density of air, κ is the von Karman constant (approximately 0.41), z_0 is an integration constant giving the virtual origin of the profile, and $f(Ri)$ is a function of the Richardson number which reflects the influence of the atmosphere condition:

$$R_i = \frac{g}{\rho_{ar}}\frac{d\rho_{ar}}{dz}\left(\frac{dU_W}{dz}\right)^{-2} \tag{2.17}$$

An important question concerns the determination of z_0 or, equivalently, of a drag coefficient C_{dW} of the surface. This is defined in terms of the mean wind velocity at a convenient height z:

$$C_{dW} = \frac{\tau_s}{\rho_{ar} U_W^2(z)} \tag{2.18}$$

For the aerodynamically rough flow, the length z_0 is approximately proportional to the friction velocity $(u^S_*)^2$, i.e.,

$$z_0 = c_W \frac{\left(u_*^S\right)^2}{g} \tag{2.19}$$

where c_W is an empirical constant.

Experimental data in natural and laboratory conditions for aerodynamically rough flow (wind velocities between 5 and 53 m/s) confirm a linear relationship between $C_{dW}^{(10)}$ and $U_W^{(10)} = U_W(10)$ as given by Massel (1989, citing earlier works in Russian by Krylov *et al.*, 1986):

$$C_{dW}^{(10)} = \left(0.71 + 0.071 U_W^{(10)}\right) 10^{-3} \tag{2.20}$$

or, in general,

$$C_{dW}^{(10)} = \left(a_W + b_W U_W^{(10)}\right) 10^{-3} \tag{2.21}$$

When the wind velocity is smaller than 5 m/s, the drag coefficient is close to the value for turbulent, aerodynamically smooth flow, and the Reynolds number $Re_x > (Re_x)_{cr}$, where $Re_x = u^S_* X_W / \nu_{ar}$. The critical value of this Reynolds number, which in coastal zones is highly dependent on the initial coastal roughness, corresponds to the situation when the viscous sublayer is destroyed and the wind waves are going to affect the wind profile. Therefore,

$$\frac{g z_0}{\left(u_*^S\right)^2} = c_{W1} \left(\frac{u_*^S}{3\sqrt{g \nu_{ar}}} \right)^{-3} \tag{2.22}$$

in which ν_{ar} is the kinematic viscosity of the air, and c_{W1} is a constant whose value is 43, according to Krylov *et al.* (1986, cited in Massel, 1989). Then

$$C_{dW} = \left[2.5 \ln\left(\frac{u_*^S z}{\nu_{ar}} \right) - 9.4 \right]^{-2} \tag{2.23}$$

In some occasions, power law profiles of the following type may also be used

$$\frac{U_W(z)}{U_W^{(10)}} \approx \left(\frac{z}{10} \right)^{\alpha_W} \tag{2.24}$$

where α_W is about 0.11.

Geernaert *et al.* (1986) proposed an empirical relationship to calculate C_{dW} which takes into account the wind speed and water depth for stable atmospheric conditions (fig. 2.2). A somewhat more general approach has been proposed by Perrie and Wang (1995a, b), incorporating information on the sea state through a wave age-dependent roughness.

The currents induced by the action of wind in shallow waters can be described by the simple analytical formulation presented in Massel (1989; from Shadrin, 1972) in which u_W, v_W and w_W show a parabolic, linear and cubic variation with depth z, respectively:

$$u_W(z) = \frac{\tau_s^x}{4\nu_V}\left(d + 4z + \frac{3z^2}{d}\right) - \frac{1}{2}\sqrt{\frac{\tau_b^x}{\rho f_c}}\left(1 - 3\frac{z^2}{d^2}\right) \tag{2.25a}$$

$$v_W(z) = \frac{\tau_s^y}{\nu_V}(d + z) + \sqrt{\frac{\tau_b^y}{\rho f_c}} \tag{2.25b}$$

$$w_W(z) = -iz\left[\frac{1}{4}\frac{\tau_s^x}{\nu_V}\left(1 - \frac{z^2}{d^2}\right) - \sqrt{\frac{\tau_b^x}{\rho f_c}}\frac{z^2}{d^3}\right] \tag{2.25c}$$

where i is the bottom slope, f_c is a friction coefficient, ρ is the density of the water, τ_s^j and τ_b^j are the j-components of the surface and bottom shear stresses and ν_V is the vertical turbulent diffusivity -taken as a constant-, and d is the water depth. The axis x and y to which equations (2.25a, b, c) are related to are defined normal and parallel to the isobaths, respectively. The surface stress can be calculated from equation (2.18), using the wind velocity at 10m height and a drag coefficient of 0.0025.

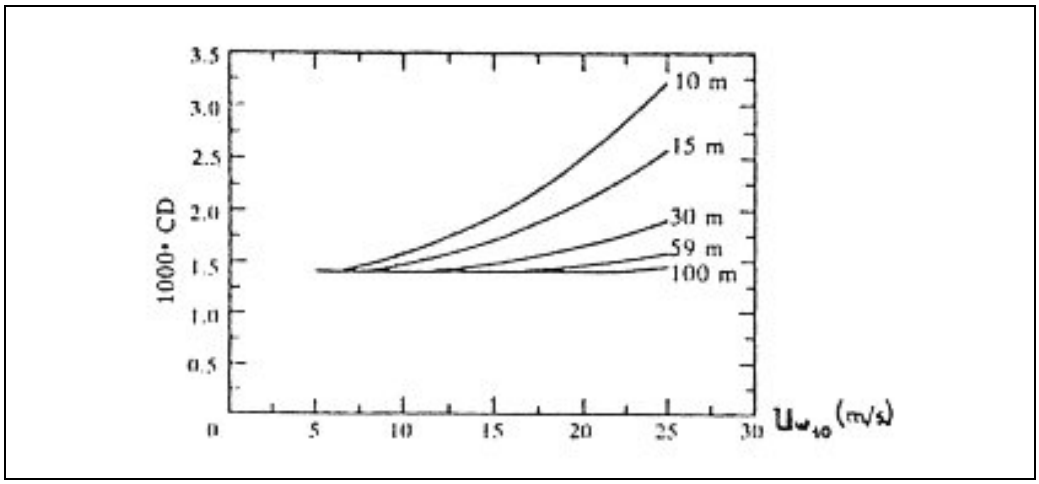

Figure 2.2: Drag coefficient C_D as a function of $V_w^{(10)}$ for five different values of the depth (from Geernaert *et al.* , 1986).

More complete alternatives are available and must be considered in cases for which equations (2.25a, b, c) become unusable. If the bathymetry is not smooth enough, or if the turbulent diffusion cannot be assumed constant, models that introduce variable ν_t should be used, thus obtaining $u_W(z)$ profiles which differ from the classical parabolic solution. Examples of these models include combinations of linear and constant profiles (Davies, 1980), linear and parabolic profiles (Wu and Tsanis, 1995), or calculate the diffusivity using high order closure models, either k-ε (Yamashita *et al.*, 1994) or k-l (Koutitas and O'Connor, 1980).

2.2.2 Oscillatory motion

The wave field is the predominant factor in coastal and, particularly, surf zone hydrodynamics. The dissipation of wave energy, mainly by wave breaking, creates stresses which induce new currents in the breaking zone, and also plays a major role in the distribution of turbulent kinetic energy.

Based on different characteristics, at least four different types of wave classification can be defined:

a) Driving / restoring forces: “tsunamis”, generated by submarine earthquakes; storm surges, generated by meteorological disturbances; wind waves, driven by the wind stress on the sea surface; and capillary waves.

b) Period: long waves, short waves.

c) Probability distribution: regular or irregular waves.

d) Symmetry: vertically / horizontally symmetric, non-symmetric.

Because of their frequent occurrence, the most important waves in coastal hydrodynamics are those generated by the wind-induced stress on the sea surface, and it is this type which shall be treated here. Tsunamis, storm surges, and gravity and capillary waves are not considered, but a description of them can be found in Pond and Pickard (1989).

Wind-induced waves can be classified into two categories, based on their predominant generation mechanism:

a) ‘Sea’ waves, associated to local wind stresses, with short periods (between 1 and 15 seconds -Svendsen and Jonsson, 1982).

b) ‘Swell’ waves, with periods from around 8 to 30 seconds, highly dependent on the characteristics of the water basin. These result from the propagation of sea waves, generated in open seas, towards coastal regions, loosing the higher frequency components, and finally presenting a fairly organised frequency distribution.

The description of waves (or wave fields) is done by specifying the values of a series of characteristic physical parameters. If the wave field is regular, these parameters are the wave height H_w, the wave period T_w and the direction of propagation θ_w. When the wave field is irregular, these physical parameters are difficult to obtain, and they are replaced by statistical parameters such as the significant wave height H_s or the directional energy spectrum.

2.2.2.1 Governing equations

At a fixed point, the governing equations for the water wave motion are the Euler equations of motion and the continuity equation (Horikawa, 1988):

$$\frac{\partial u_i}{\partial t} + u_j \frac{\partial u_i}{\partial x_j} + w \frac{\partial u_i}{\partial z} = -\frac{1}{\rho} \frac{\partial p}{\partial x_i} \tag{2.26}$$

$$\frac{\partial w}{\partial t} + u_j \frac{\partial w}{\partial x_j} + w \frac{\partial w}{\partial z} = -g - \frac{1}{\rho} \frac{\partial p}{\partial z} \tag{2.27}$$

$$\frac{\partial u_j}{\partial x_j} + \frac{\partial w}{\partial z} = 0 \tag{2.28}$$

where u_i (i=1,2) and w denote the horizontal and vertical components of the water particle velocity, g is the acceleration due to gravity, x_i (i=1,2) and z are the horizontal and vertical spatial coordinates, and t is the time. Equations (2.26) to (2.28) assume that the fluid is incompressible (i.e., ρ constant), inviscid and irrotational; where the effects of the surface or bottom boundary layer become significant, the Euler equations should be replaced by the Navier-Stokes equations of motion.

Under the assumption of irrotational flow, a velocity potential ϕ can be defined by the following equations:

$$u_i = \frac{\partial \phi}{\partial x_i}, \qquad w = \frac{\partial \phi}{\partial z} \tag{2.29}$$

and the equations of motion can then be integrated to yield the pressure equation (generalised Bernoulli equation):

$$\frac{\partial \phi}{\partial t} + \frac{1}{2}\left[\left(\frac{\partial \phi}{\partial x_i}\right)^2 + \left(\frac{\partial \phi}{\partial z}\right)^2\right] + \frac{p}{\rho} + gz = 0 \tag{2.30}$$

By substituting equation (2.29) in the continuity equation (2.28), the Laplace equation can be obtained

$$\frac{\partial^2 \phi}{\partial x^2} + \frac{\partial^2 \phi}{\partial y^2} + \frac{\partial^2 \phi}{\partial z^2} = 0 \tag{2.31}$$

which, together with (2.30), governs the surface water waves, being ϕ and p the unknowns.

The bottom and surface boundary conditions must also be stated. At the bottom (z=-h), the normal component of the water particle must be zero,

$$w = -u_i \frac{\partial h}{\partial x_i} \tag{2.32}$$

where h is the still water depth.

At the free surface, however, the boundary condition is a bit more complicated, since the boundary position (the surface elevation, η) is not known. Thus, a kinematic and a dynamic boundary conditions are imposed, expressed as

$$w = \frac{\partial \eta}{\partial t} + u_i \frac{\partial \eta}{\partial x_i} \tag{2.33}$$

$$\frac{\partial \phi}{\partial t} + \frac{1}{2}\left[\left(\frac{\partial \phi}{\partial x_i}\right)^2 + \left(\frac{\partial \phi}{\partial z}\right)^2\right] + \frac{p_a}{\rho} + g\eta = 0 \tag{2.34}$$

The kinematic boundary condition –equation (2.33)– requires that a water particle located at the free surface at a time *t* remains there, whereas the dynamic boundary condition requires that the pressure at the free surface be equal to the atmospheric pressure p_a at the surface.

The wave motion can be described by finding the velocity potential ϕ from the Laplace equation and the boundary conditions, and then obtaining the pressure from equation (2.30). The main problem lies in the fact that the free surface boundary conditions given by (2.33) and (2.34) are non-linear (since u_i, w, ϕ and η are unknown), calling for different solution methods.

a) Linear wave theories

This is the solution for the small amplitude wave problem, that is, on the assumption that the wave amplitude is small in comparison with the wavelength. If the relative wave amplitude is small, appropriately non-dimensionalised quantities of u_i, w, ϕ and η also become small quantities, and the surface boundary conditions (2.33) and (2.34) can be expanded in a Taylor series with respect to η. Eliminating η between the resulting linearised equations yields a surface boundary condition in terms only of ϕ:

$$\frac{\partial \phi}{\partial z} = -\frac{1}{g}\frac{\partial^2 \phi}{\partial t^2} \qquad (z = 0) \tag{2.35}$$

Equation (2.35), together with the linearised form of equations (2.31) and (2.32) can be used to determine the velocity potential ϕ, and the pressure p can then be found from the linearised form of equation (2.30).

Under the small amplitude assumption, and defining the x-axis along the propagation direction, ϕ becomes:

$$\phi(x,z,t) = \frac{a_w \sigma}{\mathbf{k}} \frac{\cosh[\mathbf{k}(h+z)]}{\cosh(\mathbf{k}h)} \sin[\mathbf{k}(x - c_w t)] \tag{2.36}$$

where a_w is the wave amplitude (equal to half the wave height H_w), σ is the angular frequency, **k** is the wave number and c_w is the wave celerity. Other variables can also be calculated:

a) Velocity components of the water particle:

$$u = a_w \sigma \frac{\cosh[\mathbf{k}(h+z)]}{\sinh(\mathbf{k}h)} \cos[\mathbf{k}(x - c_w t)] \tag{2.37}$$

$$w = a_w \sigma \frac{\sinh[\mathbf{k}(h+z)]}{\sinh(\mathbf{k}h)} \sin[\mathbf{k}(x - c_w t)] \tag{2.38}$$

b) Wave profile:

$$\eta = a_w \cos[\mathbf{k}(x - c_w t)] \tag{2.39}$$

c) Pressure:

$$p = \rho g a_w \frac{\cosh[\mathbf{k}(h+z)]}{\cosh(\mathbf{k}h)} \cos[\mathbf{k}(x - c_w t)] - \rho g z \tag{2.40}$$

d) Wavelength and wave celerity:

If the water depth h and the wave period T_w ($T_w = 2\pi/\sigma$) are given, the dispersion relation determines the wavelength L_w ($L_w = 2\pi/\mathbf{k}$):

$$\sigma^2 = g\mathbf{k}\tanh(\mathbf{k}h) \tag{2.41}$$

and the wave celerity is expressed as:

$$c_w = \frac{\sigma}{\mathbf{k}} = \sqrt{\frac{g}{\mathbf{k}}\tanh(\mathbf{k}h)} \tag{2.42}$$

e) Water particle trajectory:

In the first order of approximation, the particle path becomes an ellipse,

$$\frac{(x - x_o)^2}{\left\{a_w \frac{\cosh[\mathbf{k}(h+z_o)]}{\sinh(\mathbf{k}h)}\right\}^2} + \frac{(z - z_o)^2}{\left\{a_w \frac{\sinh[\mathbf{k}(h+z_o)]}{\sinh(\mathbf{k}h)}\right\}^2} = 1 \tag{2.43}$$

where (x_o, z_o) is the average particle position; in second order, the trajectory is not closed, and the particle moves in the direction of wave propagation, leading to mass transport by the waves.

f) Total energy:

$$E = E_k + E_p = \frac{\rho g a_w^2}{2} = \frac{\rho g H_w^2}{8} \tag{2.44}$$

g) Kinetic and potential energy:

$$E_k = \overline{\int_{-h}^{\eta} \frac{\rho}{2}\left(u^2 + w^2\right) dz} = \frac{\rho g H_w^2}{16} \tag{2.45}$$

$$E_p = \overline{\int_0^{\eta} \rho g z dz} = \frac{\rho g H_w^2}{16} \tag{2.46}$$

h) Mass transport:
$$M_x = \overline{\int_{-h}^{\eta} \rho u dz} = \frac{E}{c_w} \tag{2.47}$$

i) Energy flux:
$$F_x = \overline{\int_{-h}^{\eta} \left\{ p + \frac{\rho}{2}\left(u^2 + w^2\right) + \rho g z \right\} u dz} = E c_g = E c_w n \tag{2.48}$$

where
$$n = \frac{1}{2}\left(1 + \frac{2|\mathbf{k}|h}{\sinh\left(2|\mathbf{k}|h\right)} \right) \tag{2.49}$$

and c_g is the group velocity, which is the speed of energy transfer.

j) Momentum fluxes (radiation stresses; Longuet-Higgins & Stewart, 1964):

$$S_{xx} = \overline{\int_{-h}^{\eta} \left(p + \rho u^2\right) dz} - \frac{\rho g}{2} h^2 - \frac{M_x^{\ 2}}{\rho h} = E\left(2n - \frac{1}{2} \right) \tag{2.50}$$

$$S_{yy} = \overline{\int_{-h}^{\eta} p dz} - \frac{\rho g}{2} h^2 = E\left(n - \frac{1}{2} \right) \tag{2.51}$$

b) Finite amplitude wave theories

A complete analytical solution to the set of equations (2.30) to (2.34) cannot be found because of the non-linearity of the system, so one must settle for approximate solutions. One method is the perturbation approach, in which each solution is expressed as a power series in terms of a certain non-dimensional parameter, generally a function of the water depth h, the wavelength L_w and the wave height H_w. The most common perturbation solutions are the Stokes wave theory (e.g., Isobe *et al.*, 1978), valid for deep water, in which a power series in terms of H_w/L_w is obtained by using h/L_w and H_w/L_w as independent parameters; and the cnoidal wave theory (e.g., Yasuda, 1978), applicable in relatively shallow waters, that uses H_w/h and the Ursell parameter ($Ur=H_wL_w^2/h^3$) to obtain a solution. Isobe and Horikawa (1982) proved that these two theories are superior to other perturbation methods developed by making other assumptions in the selection of parameters. An alternative to perturbation approaches are the numerical solution methods, such as the stream function method of Dean (1965). Detailed descriptions of these theories can be found in Horikawa (1988).

2.2.2.2 Shallow water wave transformation

The wind-induced waves developed at the open sea propagate towards the shore, undergoing a series of transformations, the description of which presents both theoretical and experimental complications (Huntley, 1980). For practical purposes, however, the simple linear theory (or Airy

theory; Wiegel, 1964) yields a sufficiently good description of wave transformation in shallow waters, even though it adopts simplifications such as a flat sea bottom and a regular wave field of infinitesimal amplitude. The practical success of this theory has led to its application even in the case of irregular wave fields, in which each bandwidth is treated separately.

As the waves approach shallower waters, they suffer a series of transformations because of the influence of changes in the environment (bottom irregularities, decreasing depth), interactions (wave-wave, current-waves) and the presence of tides, winds, etc. This transformation process is called shoaling, and it involves changes in almost all the physical wave parameters: wave height H_w, propagation velocity c_w, group celerity c_g, and wavelength L_w. It is usually assumed that the period T_w remains unchanged until breaking occurs; afterwards, variations such as the appearance of period subharmonics take place because of non-linear effects.

When the relationship h/L_w becomes approximately 0.5, the effects of the bottom stress become important, and the direction of wave propagation changes and tends to become normal to the bathymetric lines, due to wave refraction. An additional change in the propagation direction may be caused by diffraction, in which a lateral transference of energy exists from regions with larger wave heights to regions with smaller H_w. Before this stage, the wave height distribution closely resembles a Rayleigh distribution. As the waves approach the shoreline, their horizontal symmetry is gradually lost, and their profile becomes skewed; the wave deformation generates dynamic instabilities which eventually lead to the breaking of the wave.

Under typical conditions, when the wave approaches shallower waters both the celerity and the wavelength decrease, whilst the group celerity c_g first increases up to a maximum value and then decreases again. Since the energy flux ($\propto H_w^2 c_g$) is essentially constant, the wave height must accordingly decrease first and then increase, until it reaches a maximum and the wave breaks. The variations in H_w are followed by an increase of the wave-front slope because of the differential celerity between different parts of the wave profile and the introduction of non-linear harmonics in the basic oscillatory motion. The growth in height of an individual wave cannot continue beyond a critical value γ_B for the relation $\gamma_w = H_w/h$ around 0.8; if γ_w exceeds this value, H_w will decrease in order to maintain γ_w nearly constant, between 0.6 and 1.3 (Huntley, 1980). This process contributes to a great increase in the vorticity and turbulence levels, and the wave dynamics changes abruptly due to the complexity of the turbulence transport and energy dissipation processes involved.

The breaking of waves appears when these reach a certain limiting value relative to their length or the water depth. In the surf zone (SZ), the wave energy transported from the deep ocean dissipates in the process of wave breaking, and is transformed mainly into turbulence energy. If the bottom slope decreases nearer to the shore, the breaking tends to stop and the waves recover their previous characteristics. In the final phase of wave propagation, the waves move up and down the swash zone; part of the incident energy is dissipated in this zone, whereas the rest is reflected back into the sea, generating stationary long waves.

a) Refraction

This phenomenon is the consequence of a change in wave celerity as a function of water depth, local current velocity and wave period. If the wave period is constant, the celerity of the wave depends mainly on the local water depth, while wave height has a small effect; the celerity distribution is also distorted by the presence of local currents (Horikawa, 1988).

The transformation of the wave profile because of refraction effects can be calculated using either the kinematic conservation principle or the classical geometric-optics approximation, or wave

ray theory (Sánchez-Arcilla and Lemos, 1990). In any case, it can be shown (Horikawa, 1988; Massel, 1989) that the amplitude a_w of the refracted wave is well expressed by

$$\frac{a_w}{a_{w0}} = K_r K_s \tag{2.52}$$

along a wave ray, where K_r and K_s are the refraction and shoaling coefficients, respectively, and a_{w0} is the wave amplitude in deep waters. The shoaling coefficient is defined as

$$K_s = \sqrt{\frac{c_{g_0}}{c_g}} \tag{2.53}$$

whereas the refraction coefficient is

$$K_r = \sqrt{\frac{b_0}{b}} \tag{2.54}$$

with b, b_0 equal to the separation between neighbouring wave rays, or

$$K_r = \sqrt{\frac{\cos\alpha_{w0}}{\cos\alpha_w}} \tag{2.55}$$

where α_{w0} and α_w are the initial and refracted incidence angles, respectively, for the case of a straight parallel bottom. When the bathymetry is arbitrary, the ray spacing must be obtained from differential equations like those found in Dean and Darlymple (1984) or Horikawa (1988).

b) Diffraction

Diffraction is the phenomenon by which diffusion or transverse flow of wave energy exists, resulting in the propagation of waves into sheltered basins.

The wave ray theory used to estimate the effects of wave refraction excludes diffraction, and is thus unable to predict wave characteristics near coastal structures. Even though a diffraction coefficient K_{df} can be defined in some cases (e.g., Penney and Price, 1952), the combined refraction-diffraction problem should be formulated to include the effects of diffraction.

A particularly significant way of approaching this problem is by introducing the mild-slope equation, which results from eliminating the vertical coordinate from the basic wave motion equation (2.31) in cases where bottom slopes are gentle. A complete analysis of the mild-slope equation theory can be found elsewhere (Horikawa, 1988; Sánchez-Arcilla and Lemos, 1990; Massel, 1989) and therefore will not be given here.

c) Wave breaking

Waves can break following four different patterns, namely *spilling*, *plunging*, *collapsing*, and *surging* (fig. 2.3):

a) Spilling*:* This wave breaking pattern is characterised by the appearance of foam, air bubbles and turbulent water on the wave crest, which can eventually cover the whole wave front. The breaking is set off when a portion of the wave moves forward faster then the remaining part.

b) Plunging*:* The wave crest moves faster than the rest of the wave, leading to a steepening and overturning of the wave front, which plunges into the water ahead.

c) Collapsing*:* It is a pattern similar to that of plunging waves, but with overturning occurring not at the point of maximum height, but below.

d) Surging: The wave crest and the wave front evolve in a smooth manner, generating little foam and bubbles when breaking.

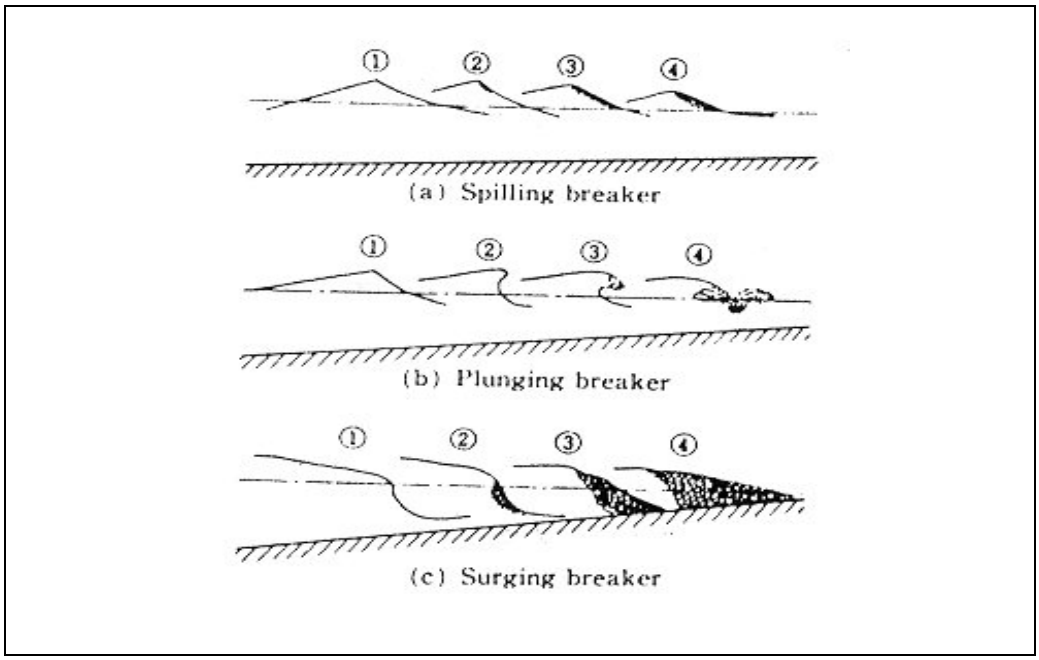

Figure 2.3: Schematic patterns of wave breaking (from Horikawa, 1988).

c.1) Breaking criteria

The most extended criterion for predicting wave breaking states that collapse will occur if the parameter γ_w, defined as

$$\gamma_w = \frac{H_w}{h} \tag{2.56}$$

becomes larger than a critical value γ_B. Theoretical studies of solitary waves and several laboratory measurements of regular wave fields have given values of γ_B between 0.73 and 1.0, with a typical value of 0.78, but field measurements show a larger dispersion (from 0.5 to 1.1), so equation (2.56) must be used with care. In any case, the use of (2.56) is restricted to nearly monotonically decreasing

depth, since it implies that the wave height must increase after breaking if the depth increases, in disagreement with observations.

Battjes and Janssen (1978) developed a criterion for defining irregular waves through a critical value H_{wM} of the wave height. According to their theory, wave breaking will appear when the wave height becomes larger than H_{wM}, given by the following expression:

$$H_{wM} = \frac{0.88}{k}\tanh\left(\frac{\gamma kh}{0.88}\right) \tag{2.57}$$

The breaking type can be quantitatively estimated using the Iribarren non-dimensional parameter (Irribarren and Nogales, 1949)

$$\xi_0 = i\left(L_{w0} / H_{w0}\right)^{-0.5} \tag{2.58}$$

or a modified local parameter ξ_B defined using the wave height at breaking point H_{wB} instead of H_{w0}. An alternative parameter has been defined by Yoo (1986), as a function of local variables, including the bottom slope. This parameter, β_Y, is defined as

$$\beta_Y = \frac{\xi_B^2}{\pi k h_B} \tag{2.59}$$

where k is the local wave number $2\pi/L_{wB}$, h_B is the breaker depth, and L_{wB} is the wavelength at breaking point. According to these parameters, the different breaking types are defined by

- spilling, if $\xi_B < 0.4$ or $\xi_0 < 0.46$, or $\beta_Y < 0.2$
- plunging, if $0.46 < \xi_B < 2.0$, or $0.2 < \beta_Y < 2.1$
- collapsing, if $\xi_B > 2.0$ or $\xi_0 > 3.3$, , or $\beta_Y > 2.1$

c.2) Breaking wave height

Several criteria exist to predict the wave height at breaking point, both for regular and irregular wave fields. All of the proposed expressions fall into two groups: in the first, only local parameters at the breaking point, such as the wave period and length, and the water depth, are relevant, while the second group relates the wave conditions in deep waters and those at the breaker.

Hamada (1951) proposed the following relationship

$$\frac{H_{wB}}{L_{wB}} = 0.142\tanh\left(\frac{2\pi h_B}{L_{wB}}\right) \tag{2.60}$$

in which H_{wB} is the breaking wave height. This equation, however, does not include the bottom slope, and cannot be used in general situations.

The inclusion of the beach slope (i) in equation (2.60) leads to (Ostendorf & Madsen, 1979):

$$\frac{H_{wB}}{L_{wB}} = 0.14\tanh\left\{(0.8+5\tan(i))\frac{2\pi h_B}{L_{wB}}\right\}\tan(i)<0.1$$

$$\frac{H_{wB}}{L_{wB}} = 0.14\tanh\left\{1.3\frac{2\pi h_B}{L_{wB}}\right\}\tan(i)>0.1 \qquad (2.61)$$

where L_{wB} has to be calculated from the dispersion relation for small amplitude wave theory. Another criterion -empirical- was given by Sunamura (1983), from results obtained in large wave flumes, also considering the bottom slope:

$$\frac{H_{wB}}{h_B} = 1.09(\tan(i))^{0.19}\left(\frac{h_B}{L_{wB}}\right)^{-0.1} \qquad (2.62)$$

Examples of the second group of breaking expressions are those given by Munk (1949), Komar and Gaughan (1973), Le Mehauté and Koh (1967) or Sunamura (1983) - equations (2.63), (2.64) , (2.65), and (2.66), respectively-:

$$\frac{H_{wB}}{H_{w0}} = \frac{1}{3.3(H_{w0}/L_{w0})^{0.33}} \qquad (2.63)$$

$$\frac{H_{wB}}{H_{w0}} = 0.563(H_{w0}/L_{w0})^{1/5} \qquad (2.64)$$

$$\frac{H_{wB}}{H'_{w0}} = 0.76(\tan(i))^{1/7}(H'_{w0}/L_{w0})^{-1/4} \qquad (2.65)$$

$$\frac{H_{wB}}{H_{w0}} = (\tan(i))^{1/5}(H_{w0}/L_{w0})^{-1/4} \qquad (2.66)$$

where L_{w0} and H_{w0} are the wave length and height in deep waters, and H'_{w0} is the corrected deep water height, given by $K_rK_dK_{df}H_0$, where K_r, K_d, and K_{df} are refraction and diffraction coefficients, and wave height dissipation rate due to friction, respectively.

For irregular wave fields, the wave height at the breaker has been studied by Battjes and Stive (1985) who proposed the following expression

$$\frac{H_{wB,rms}}{h_B} = 0.5+0.4\tanh\left(33\frac{H_{w0}}{L_{w0}}\right) \qquad (2.67)$$

based on numerous field and laboratory data, and with different bottom profiles. Nairn (1990) modified equation (2.67) to include new data, and obtained

$$\frac{H_{wB,rms}}{h_B} = 0.39+0.57\tanh\left(33\frac{H_{w0}}{L_{w0}}\right) \qquad (2.68)$$

2.2.3 Nearshore currents

The obvious effect of wind stress on the surface of the sea is the production of a steady movement of the water surface layer in the same general direction as the wind. This movement, however, will be restricted in the proximity of a coast line, leading to a rising water level (set-up) and to the development of surface slopes which may extend away from the coast. The surface slopes produce a horizontal pressure gradient in the water, and this in turn will generate the so-called gradient currents. The wave-induced current that flows alongshore is called longshore current, and is confined between the first breaker and the shoreline; its typical velocity values are under 1 m/s, and the highest values are observed at the breaker line (Massel, 1989).

Another wave-induced current motion is the so-called mass transport. This is a second order effect, so the velocity of the current increases rapidly with wave height. The flow across the surf zone produces a tilt of the mean water surface from the breakers to the shore. Also longshore variations in the breakers height create gradients of the mean water level within the surf zone that generate currents flowing from positions of highest breaker height to positions of lowest breaker. Here, the longshore currents converge and turn out seaward as rip currents. These currents are narrow strong return flows directed through the surf to the sea. Together with longshore currents they create a two-dimensional coastal current system within and beyond the surf zone. A series of rip currents is usually found along the coast with longshore currents feeding the rips and forming independent circulation cells.

Finally, the gravitational attraction of the moon and the sun generate the tides, and the tidal currents associated with the subsequent rising and falling of the sea surface. The relation between the elevation and the currents is straightforward in gulfs and estuaries, but becomes less clear off an open coast or away from the land. Tidal currents will be treated later in §2.2.5.

2.2.3.1 Radiation stress concept

The radiation stress principle was first derived by Longuet-Higgins and Stewart (1962) using both the mass and momentum conservation equation, and will be used here to develop the expressions for the coastal phenomena associated with longshore current profiles, and nearshore circulation systems and rip currents.

The time-average value of the total flux of horizontal momentum across a vertical plane, minus the force resulting from the still water hydrostatic pressure, when a wave propagates in the *x* direction, can be expressed as

$$S_{XX} = \overline{\int_{-h}^{\eta} \left(p + \rho u_{orb}^2\right) dz} - \int_{-h}^{0} p_0 dz \tag{2.69}$$

where p_0 is a still water hydrostatic pressure. Equation (2.69) can be re-written as (Basco, 1982)

$$S_{XX} = \int_{-h}^{0} \overline{\rho\left(u_{orb}^2 - w_{orb}^2\right)} dz + \frac{1}{2}\rho g \overline{\eta^2} \tag{2.70}$$

and the analogous transverse stress component can be defined as

$$S_{YY} = \int_{-h}^{0} \overline{\rho w_{orb}^2} dz + \frac{1}{2}\rho g \overline{\eta^2} \tag{2.71}$$

Since the orbital velocity v_{orb} in the Y direction (parallel to the wave crests) is zero, the shear component S_{XY} vanishes

$$S_{XY} = \overline{\int_{-h}^{\eta} \rho u_{orb} v_{orb} dz} = 0 \tag{2.72}$$

It is convenient to write the radiation stress components in a new coordinate system in which the x-component is normal to the shoreline and the y-component is in the longshore direction:

$$\begin{aligned} S_{xx} &= \frac{1}{2}(S_{XX} + S_{YY}) - \frac{1}{2}(S_{XX} - S_{YY})\cos 2\alpha_w \\ S_{yy} &= \frac{1}{2}(S_{XX} - S_{YY}) + \frac{1}{2}(S_{XX} + S_{YY})\cos 2\alpha_w \\ S_{xy} &= \frac{1}{2}(S_{XX} - S_{YY})\sin 2\alpha_w \end{aligned} \tag{2.73}$$

where α_w is the angle of wave incidence, and S_{xy} is the shear stress component in the longshore direction due to the excess momentum flux of oblique incidence.

By substituting the particle orbital velocities u_{orb} and w_{orb} and surface elevation η given by the linear wave theory, equations (2.70), (2.71), and (2.73) can be written as functions of the total wave energy E:

$$\begin{aligned} S_{XX} &= E\left(2n - \frac{1}{2}\right) \\ S_{YY} &= E\left(n - \frac{1}{2}\right) \end{aligned} \tag{2.74}$$

$$\begin{aligned} S_{xx} &= E\left(\frac{3}{2}n - \frac{1}{2}\right) - \frac{1}{2}En\cos 2\alpha_w \\ S_{yy} &= E\left(\frac{3}{2}n - \frac{1}{2}\right) + \frac{1}{2}En\cos 2\alpha_w \\ S_{xx} &= En\sin\alpha_w \cos\alpha_w \end{aligned} \tag{2.75}$$

where $$n = \frac{1}{2}\left(1 + \frac{2|\mathbf{k}|h}{\sinh(2|\mathbf{k}|h)}\right) \tag{2.76}$$

2.2.3.2 Longshore currents

A large number of factors influence longshore currents, but the complexity of the forcing field, the geometry and the fluid must be reduced in order to allow for a theoretical treatment. Under certain simplifying assumptions, there is a balance of forces such that:

driving force + bottom friction + lateral friction = 0

For a plane, infinite beach, even though the gradient of the longshore radiation stress component is zero, there is a net mean flux of *y*-momentum due to the waves because of S_{xy}. This driving stress in the longshore direction is resisted by the bottom shear stress τ_b^x and by the lateral shear force over the total depth due to turbulent mixing, F_{L^*}. The momentum balance in the *y* direction then becomes, according to Longuet-Higgins (1970):

$$\frac{\partial S_{xy}}{\partial x} - \tau_b^x + \frac{dF_{L^*}}{dx} = 0 \tag{2.77}$$

The longshore velocity component appears included both in the bottom shear stress term τ_b^x and in the lateral shear force term F_{L^*}.

Several models have been developed to reproduce longshore current profiles. The first model proposed by Longuet-Higgins (1970) essentially neglected cross-shore effects such as the set-up, and assumed small longshore currents and wave incidence angles in order to linearise the bed shear stress term. The later model of Kraus and Sasaki (1979) is similar to Longuet-Higgins's and includes the effects of non-normal wave incidence, but their conclusions are the same as in the previous model.

Neglecting the turbulent mixing, Longuet-Higgins (1970) obtained a longshore velocity profile in the form

$$u_0 = \frac{h}{h_B}\begin{cases} \dfrac{5\pi\gamma_w}{16 f_{wc}}(g h_B)^{1/2} i \sin\alpha_{wB} & h \le h_B \\ 0 & h > h_B \end{cases} \tag{2.78}$$

where f_{wc} is a wave-current friction factor of order 10^{-2} (Sánchez-Arcilla and Lemos, 1990), and α_{wB} is the wave incidence angle at the breaker.

When the turbulent mixing is introduced, the expression for the profile becomes somewhat more complicated, and is given by

$$u^* = \begin{cases} B_1 x^{*P_1} + A x^* & 0 < x^* < 1 \\ B_2 x^{*P_2} & 1 < x^* < \infty \end{cases} \qquad (P \neq 2/5) \qquad (2.79)$$

$$u^* = \begin{cases} \frac{10}{49} x^* - \frac{5}{7} x^* \ln x^* & 0 < x^* < 1 \\ \frac{10}{49} x^{*-\frac{5}{2}} & 1 < x^* < \infty \end{cases} \qquad (P = 2/5) \qquad (2.80)$$

where x^* and u^* are dimensionless distances and velocities (equal to x/x_B and u/u_0, respectively), and the variables P, P_1, P_2, A_1, B_1, and B_2 are defined as follows:

$$P = \frac{\pi A_2 i}{\gamma_w f_{wc}} \qquad (2.81)$$

$$P_1 = -\frac{3}{4} + \left(\frac{9}{16} + \frac{1}{P} \right)^{1/2} \qquad (2.82)$$

$$P_2 = -\frac{3}{4} - \left(\frac{9}{16} + \frac{1}{P} \right)^{1/2} \qquad (2.83)$$

$$A_1 = -\frac{1}{1 - 5P/2} \qquad (2.84)$$

$$B_1 = \left(P(1 - P_1)(P_1 - P_2) \right)^{-1} \qquad (2.85)$$

$$B_2 = \left(P(1 - P_2)(P_1 - P_2) \right)^{-1} \qquad (2.86)$$

and A_2 is a dimensional coefficient between 0 and 0.016 (Longuet-Higgins, 1970). Figure 2.4 shows the form of the current profiles as given by equation (2.79) for a sequence of values of the mixing parameter P.

Detailed descriptions of other longshore current models, such as the one presented by Kraus and Sasaki (1979) or the one by Thornton and Guza (1986), can be found in Sánchez-Arcilla and Lemos (1990).

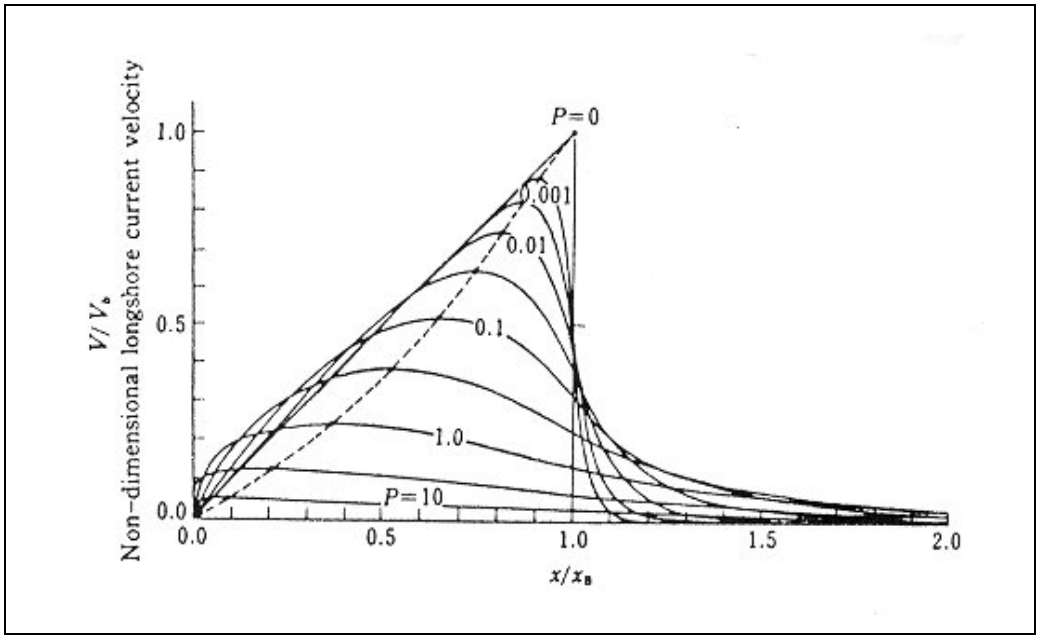

Figure 2.4: Longshore current profiles for different values of the turbulent mixing parameter *P* (from Longuet-Higgins, 1970).

2.2.3.3 Rip currents

The existence of longitudinal gradients of the wave height generate mean water level gradients inside the surf zone which create a water displacement from regions with high H_w to regions with smaller wave heights. This effect can result in the convergence of the longshore currents at the points of small H_w, and this in turn can generate seaward currents, called rip currents.

The mechanisms which originate the longitudinal wave height gradients can be classified according to several authors (Sasaki, 1978; Horikawa, 1988) into two main types:

a) Longitudinal variations of the external force, which may be either the wave radiation stress tensor (Noda, 1974), edge waves (Bowen, 1969), infragravity waves (Bowen and Inman, 1969), cross waves (Dalrymple, 1975), bottom topography irregularities (Sonu, 1972) or diffracted waves (Liu and Mei, 1974).

b) Hydrodynamic instabilities, first proposed by Hino (1973) and studied later by other authors.

The theoretical treatment of rip currents, valid for the steady state, presented by Bowen (1969) is here described. If the stream function ψ is defined as

$$\mathrm{ud} = \frac{\partial \psi}{\partial \mathrm{y}}$$

$$\mathrm{vd} = -\frac{\partial \psi}{\partial \mathrm{x}} \qquad (2.87)$$

and the corresponding momentum conservation equations are adequately treated (i.e., the convective and diffusive terms neglected and a linear bottom stress assumed) the following vorticity (Ω) equations can be obtained:

$$\frac{\partial\psi}{\partial y}\frac{\partial}{\partial x}\left(\frac{\Omega}{d}\right)-\frac{\partial\psi}{\partial x}\frac{\partial}{\partial y}\left(\frac{\Omega}{d}\right)=\frac{\partial}{\partial x}\left(\frac{\tau_b^y}{\rho d}\right)-\frac{\partial}{\partial y}\left(\frac{\tau_b^x}{\rho d}\right)+ \\ +\frac{\partial}{\partial x}\left\{\frac{1}{\rho d}\left(\frac{\partial S_{yy}}{\partial y}+\frac{\partial S_{yx}}{\partial x}\right)\right\}-\frac{\partial}{\partial y}\left\{\frac{1}{\rho d}\left(\frac{\partial S_{xx}}{\partial x}+\frac{\partial S_{xy}}{\partial y}\right)\right\} \tag{2.88}$$

$$\Omega=\frac{1}{d}\left(\frac{\partial^2\psi}{\partial x^2}+\frac{\partial^2\psi}{\partial y^2}\right)-\frac{1}{d^2}\left(\frac{\partial\psi}{\partial x}\frac{\partial d}{\partial x}+\frac{\partial\psi}{\partial y}\frac{\partial d}{\partial y}\right) \tag{2.89}$$

The linear analytical solution to these equations, including the bottom friction, is shown in figure 2.5 (from Horikawa, 1988), where it can be seen that a rip current arises in the region of low waves which is in the neighbourhood of $\lambda y=\pi$. The varying wave height generates a clockwise circulation pattern.

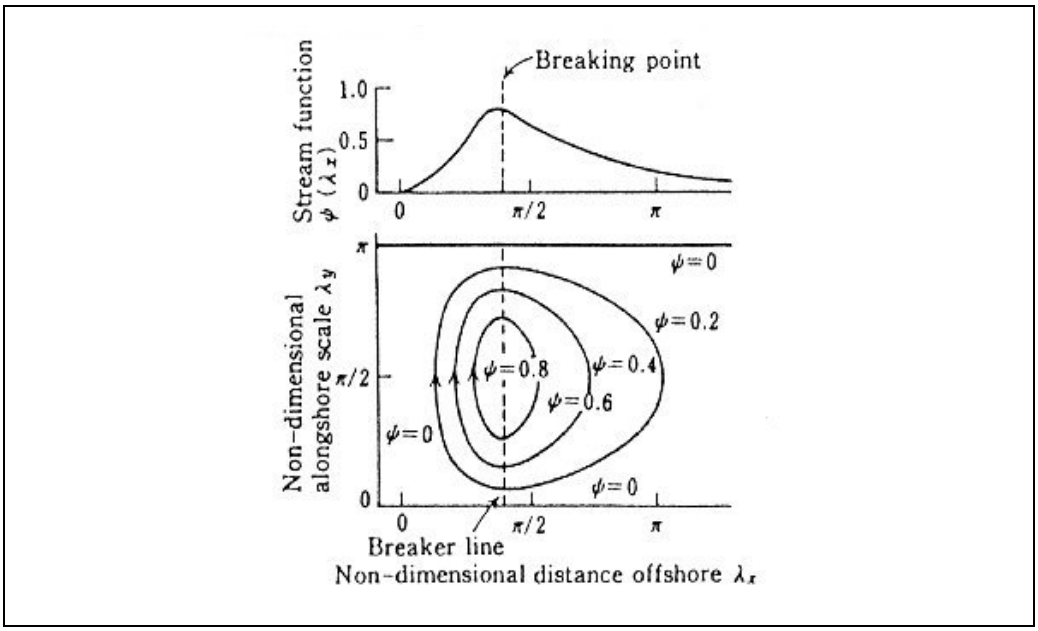

Figure 2.5: Linear solution of nearshore circulation pattern including bottom friction, following Bowen's (1969) model (from Horikawa, 1988).

A more realistic rip current flow pattern was obtained by the same author when he included the effects of horizontal mixing in the solution, numerically solving the following non-linear equation

$$\frac{\partial\psi}{\partial y}\frac{\partial}{\partial x}\left(\frac{\Omega}{d}\right)-\frac{\partial\psi}{\partial x}\frac{\partial}{\partial y}\left(\frac{\Omega}{d}\right)+\nu_H\left(\frac{\partial^2\Omega}{\partial x^2}+\frac{\partial^2\Omega}{\partial y^2}\right)=-B\sin\lambda y \tag{2.90}$$

where ν_H is the horizontal turbulent diffusion coefficient, and the term on the right hand side is the forcing term. With this solution, the width of the rip current is narrower compared with that from the linear solution, and the current speed is stronger.

The separation between rips is highly variable, and values ranging from 30m to 400m have been reported; the width of the rip currents may vary between 10m and 30m in the regions of the rip head (Massel, 1989). The estimation of the rip separation can be done with a number of different formulations, like that proposed by Bowen (1969) for the case of a longitudinal variation of the wave height induced by standing edge waves:

$$L_{rip} = \frac{T_w^2 g}{2\pi}\sin(2n+1)i \tag{2.91}$$

where n is the mode of the edge waves. A different expression has been proposed by Dalrymple (1978) as

$$\lambda x_B = \frac{1}{A_D} + 2.8 \tag{2.92}$$

where $\lambda=2\pi/L_{rip}$, and A_D is the Dalrymple-Lozano parameter, defined as

$$A_D = \frac{\gamma_B \tan(i)}{64\, f_{wc}} \tag{2.93}$$

with $\gamma_B=H_{wB}/h$, and where f_{wc} is a wave-current friction coefficient.

Hino (1974), in a different approach, treated the rip current generation mechanism as a linear instability problem. He found that the optimum rip spacing is approximately equal to $4x_B$, which is in agreement with experimental observations by Sasaki and Horikawa (1975), as can be seen in figure 2.6.

2.2.3.4 Undertow

The undertow current is a seaward return flow under wave trough level, generated by the vertical asymmetry (non-uniformity) of the wave radiation stress, which is accompanied by an important water volume carried towards the shore between wave crest and trough level.

Undertow currents balance the mass flux carried shorewards by wave breaking, including the effect of the roller (i.e., the recirculating water mass in the front face of a broken wave). This mass flux significantly increases the vertical non-uniformity of the wave radiation stress, with much higher values between wave trough and crest level. The dynamic balance for undertow is

$$\left\langle (\text{wave radiation stress}) + (\text{set}-\text{up}) + \begin{pmatrix} \text{horizontal turbulent tension} \\ \text{due} \\ \text{to vertical non}-\text{uniformity} \end{pmatrix} \right\rangle = 0 \tag{2.94}$$

where <·> denotes averaging over wave and turbulence timescales; this relationship is valid both depth-integrated or at a given *z*-level below trough level.

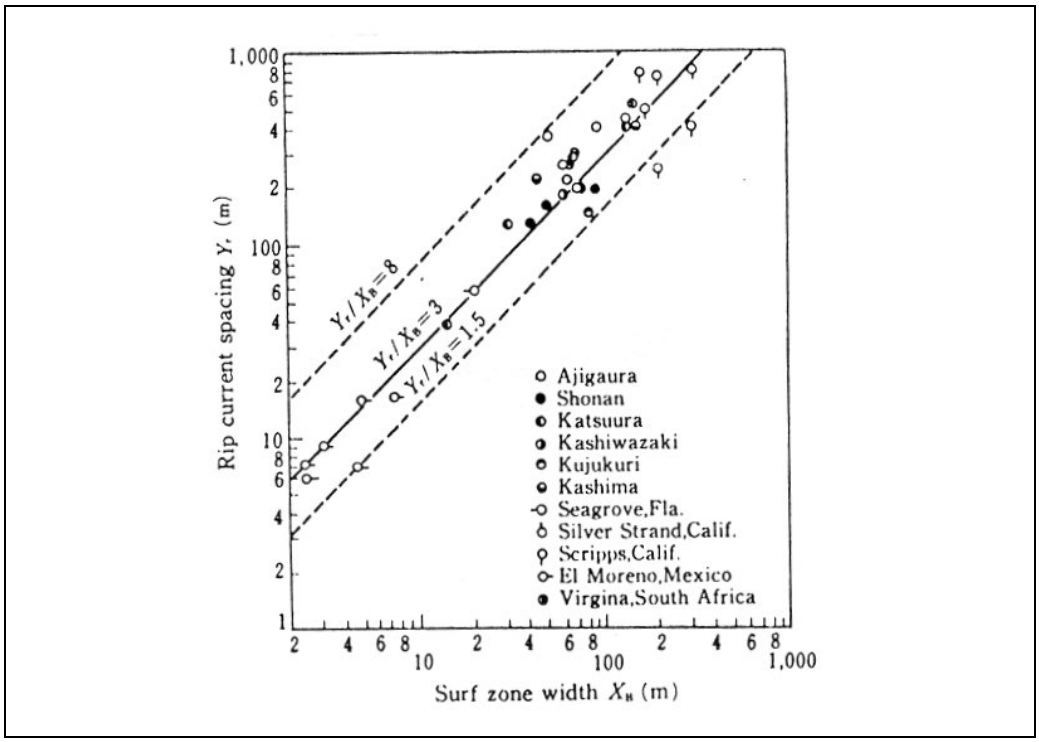

Figure 2.6: Rip current separation as a function of the surf zone width, from Horikawa (1988).

The values of the undertow can be found by comparing the equation resulting from applying the operator <·> to the cross-shore momentum equation, and assuming the motion as steady with the depth-integrated and time averaged momentum balance. Eliminating the hydrostatic pressure gradient and assuming that any vertical asymmetry in the wave radiation stress must be balanced by an internal turbulent stress, the following equation is obtained

$$\frac{\partial}{\partial x}\left(\left\langle u_{orb}^2\right\rangle-\left\langle w_{orb}^2\right\rangle\right)+g\frac{\partial}{\partial x}\langle\eta\rangle+\frac{\partial}{\partial z}\langle u_{orb}w_{orb}\rangle=\frac{\partial}{\partial z}\left(\nu_V\frac{\partial u(x,z)}{\partial z}\right) \qquad (2.95)$$

The solution of equation (2.95) requires the knowledge of the right-hand side terms, of the boundary conditions, and of the vertical distribution of the turbulent viscosity ν_V. The variation of ν_V with depth has not been well established yet: Smith and Svendsen (1985) assume a constant viscosity, Deigaard *et al.* (1991) use the expression $\nu_V \approx z^{3/2}$, and Sánchez-Arcilla *et al.* (1992) use a parabolic profile based on experimental data presented by Okayasu (1989) and confirmed by Rodriguez (1997).

If both the eddy viscosity and the wave stress $\left\langle u_{orb}^2\right\rangle-\left\langle w_{orb}^2\right\rangle$ are assumed independent of *t* and *z*, and since the term in $\langle\eta\rangle$ is also *z*-independent, the undertow current velocity *u* is found to be

$$u(z) = \frac{z^2}{2\rho\nu_V}\frac{dR}{dx} + \frac{C_1}{\rho\nu_V}z + C_2$$
$$R = g\langle\eta\rangle + \left(\left\langle u_{orb}^2\right\rangle - \left\langle w_{orb}^2\right\rangle\right) \tag{2.96}$$

where C_1 and C_2 must be determined from the boundary conditions.

2.2.3.5 Wave-current interaction

In real situations, the wave field propagates in a flowing fluid, and the waves become affected and modified by the existing currents. The interaction between waves and currents is of great importance in sediment transport, ship navigation and forces acting on sea structures and plumes.

The problem of currents interacting with short waves is equivalent to that of wave propagation in a heterogeneous, anisotropic, dispersive and dissipative moving medium (Massel, 1989). The variations of a non-steady and non-uniform current can change all the parameters describing a wave train: if waves propagate onto a faster or slower flow, the frequency will remain constant, but the wavelength will either increase or decrease. If the waves propagate at an angle with the currents, a change in the currents will produce the refraction of the waves and the transfer of energy between the waves and the current.

The most general expression of the dynamics of a wave train in moving media is the action conservation principle. Defining the wave action as E/σ, where σ is the intrinsic frequency, this conservation principle can be written as:

$$\frac{\partial}{\partial t}\left(\frac{E}{\sigma}\right) + \nabla\left(\frac{E}{\sigma}\left(\mathbf{u} + c_g\right)\right) = 0 \tag{2.97}$$

where $\boldsymbol{u}$ is the water velocity. When the mean velocity $\boldsymbol{u}$ is not uniform there is, in general, an energy exchange between the wave train and the mean flow. From equation (2.97),

$$\frac{\partial E}{\partial t} + \nabla\left(E\left(\mathbf{u} + c_g\right)\right) = \frac{E}{\sigma}\left(\frac{\partial\sigma}{\partial t} + \left(\mathbf{u} + c_g\right)\cdot\nabla\sigma\right) \tag{2.98}$$

Assuming that the dispersion relation can depend on local properties –f_{loc}- such as the water depth, the action conservation equation can be expressed (Phillips, 1977) as

$$\frac{\partial E}{\partial t} + \nabla\left(E\left(\mathbf{u} + c_g\right)\right) + \frac{E}{\sigma}\left(\mathbf{k}\cdot\left(c_g\cdot\nabla\right)\mathbf{u} - \frac{\partial\sigma}{\partial f_{loc}}\left(\frac{\partial f_{loc}}{\partial t} + \mathbf{u}\nabla f_{loc}\right)\right) = 0 \tag{2.99}$$

where the two first terms represent the local rate of change of the wave energy density and the divergence of the energy flux, while the last term describes the interaction with the mean flow, its specific form depending on the type of wave motion under consideration.

A number of different examples, including waves propagating on currents varying in the horizontal plane, can be found in Massel (1989). In the simple case of a slowly varying current, he gives the following expressions for the absolute group velocity and the wave ray direction:

$$\mathbf{c}_g^{(a)} = \mathbf{u} + \mathbf{c}_g$$

$$\tan(\theta_{wc}) = \frac{|\mathbf{u}|\sin(\delta) + |\mathbf{c_g}|\sin(\alpha_w)}{|\mathbf{u}|\cos(\delta) + |\mathbf{c_g}|\cos(\alpha_w)} \tag{2.100}$$

where δ is the angle between the current line and the *x*-axis, and θ_{wc} is the wave propagation angle resulting from the wave-current interaction.

2.2.4 Turbulence

In any waterbody, the movement of each water particle is determined by the sum of a regular component (of velocity) and a non-regular one. The regular part is due to wave effects, currents and, in general, to all factors which occur in a fairly narrow band of frequencies and wave numbers, and are predictable at least in a statistical manner (Zeidler, 1976). All the remaining effects are included in the non-regular turbulent part.

Turbulence is generated by the appearance of instabilities in the water flow. As will be seen below, it needs a constant supply of energy to maintain itself, therefore depending on the surrounding flow. A common source of energy is the shear present in the mean flow, due either to velocity differences across fluid layers or to boundary (e.g., sea bed) friction.

It manifests itself as apparently random fluctuations of physical variables (velocity, pressure, concentration), and can only be studied using a statistical description, i.e., by formulating its behaviour in terms of average quantities which can be repeated from experiment to experiment. To statistically describe a turbulent flow, the field of physical variables is divided into mean and fluctuating parts, and the equations are averaged over a time interval large compared with the turbulent time scales. In the resulting equations, new terms appear which include correlations between different variable fluctuations. This procedure is followed in §2.1, and will not be repeated here.

In oceanic waters, fluctuations can be found ranging from length scales between 0.03 cm and 1 cm (approximately), corresponding to variations controlled by molecular forces, to those limited by the physical boundaries of the seas, which may reach length scales of up to 10,000 km. The spectrum of marine turbulence is usually wider than the spectra of other hydrodynamic phenomena such as turbulent jets, wakes, etc., both in frequency and wave number, owing to the different sources which supply energy to the flow (Zeidler, 1976).

One method of discovering the time scales associated with turbulent motion is the Fourier analysis of experimental data, which yields the turbulence energy spectrum. To define the energy spectrum $\phi_E(\omega)$, it is first necessary to introduce the concept of (auto)correlation and the correlation coefficient.

Correlation measurements give information about velocity fluctuations at different points or times. The correlation between two velocity fluctuations u'_1 and u'_2 is defined by $\overline{u'_1 u'_2}$, and the correlation coefficient is

$$R = \frac{\overline{u'_1 u'_2}}{\left(\overline{u'^2_1}\,\overline{u'^2_2}\right)^{1/2}} \tag{2.101}$$

The fluctuations u'_1 and u'_2 can be different components of the velocity at a single point, or values of the same velocity component at different times. In the latter case, $R=R(s_{\Delta t})$, where $s_{\Delta t}$ is the time delay between successive measurements.

The frequency energy spectrum is then defined as the Fourier transform of the autocorrelation (Tritton, 1988):

$$\overline{u'^2} R(s_{\Delta t}) = \int_0^\infty \phi_E(\omega) e^{i\omega s_{\Delta t}} d\omega \tag{2.102}$$

where ω is the fluctuation frequency. The energy spectrum can be interpreted as the contribution from frequency ω to the energy of the turbulence, as can be seen by setting $s_{\Delta t} = 0$ in (2.102) and recalling that the turbulent energy is proportional to $\overline{u'^2}$.

Alternatively, one may define the wave number energy spectra, indicating the distribution of energy over different length scales, as $E(|\boldsymbol{k}|)$, such that

$$\frac{1}{2}\left(\overline{u'^2} + \overline{v'^2} + \overline{w'^2}\right) = \int_0^\infty E(|\mathbf{k}|) d\mathbf{k} \tag{2.103}$$

When turbulent motion is viewed as the result of interacting motions on different length scales (eddies), the spectrum may be interpreted in terms of the energy associated with eddies of various sizes.

Since the energy input from external sources becomes important only at certain wave numbers, turbulent eddies may be classified according to their bands of energy input. So, the turbulent eddies comprised between the smallest and those with characteristic scales smaller than 100 m and of the order of 10 sec, corresponding to the energy input band associated with wind waves and swell, belong to the fine turbulence range. The following interval stretches up to scales of the order of 10 km and a few days, corresponding to tidal or inertial oscillations, and is called mesoturbulence. The largest eddies are contained in the macroturbulence range, fed by global circulation.

The energy of the external sources is fed into the largest eddies in each range, which in turn lose it to a cascade of smaller turbulent eddies, and so on, until the energy reaches the smallest eddies, characterised by the Kolmogorov lengthscale - $l_K = (\nu^3/\varepsilon)^{1/4}$ -, and is then dissipated into heat by molecular stresses. This energy cascade is described by the following equation (Tritton, 1988):

$$\frac{\partial E(|\mathbf{k}|, t)}{\partial t} = F(|\mathbf{k}|, t) - 2\nu|\mathbf{k}|^2 E(|\mathbf{k}|, t) \tag{2.104}$$

where the term on the left represents the rate of change of the energy associated with wavenumber $\boldsymbol{k}$, the second term on the right is the energy dissipation (involving ν), and $F(|\mathbf{k}|, t)$ represents the transfer of energy between wave numbers.

From dimensional analysis, supported by extensive experimental data, it has been found that the energy spectrum of oceanic turbulence is

$$E(|\mathbf{k}|) = c_3 \varepsilon^{2/3} |\mathbf{k}|^{-5/3} \qquad (2.105)$$

after assuming isotropic turbulence, i.e., that the energy transferred to an eddy from a larger one is balanced by the outflow of energy to smaller eddies. This equation is valid only for the inertial subrange, in which the effects of viscosity are negligible. Outside this range, in the upper part of the spectrum (i.e., smaller eddies), viscosity becomes important and the spectrum E will be a general function of $\boldsymbol{k}$, ε and the viscosity ν. Figure 2.7 shows one of such spectra, with peaks corresponding to the input of additional energy from external sources

The physical process corresponding to the turbulent diffusion is a primary mixing agent in coastal waters. The study and understanding of turbulence, therefore, becomes a key factor in order to evaluate the overall substance dispersion.

The spatial structure of the concentration field in a turbulent flow presents a vast variation of length scales, ranging from the pollutant microscale -O(10^{-4}m)- to the maximum length scale which characterises the waterbody. In every time or space "realisation", the concentration will show random variations associated to these spatial and temporal variations that can be up to 10^{-2} sec. In other words, the concentration field distortions are produced mainly by velocity fluctuations which are directly related to the scale of the turbulent vortices. The main role of the latter is to transfer matter between current lines. The field of advective velocities defines a set of nearly stationary current lines, and it is the differences in velocity of these lines which give rise to longitudinal dispersion, as will be seen in §2.3.1.2.

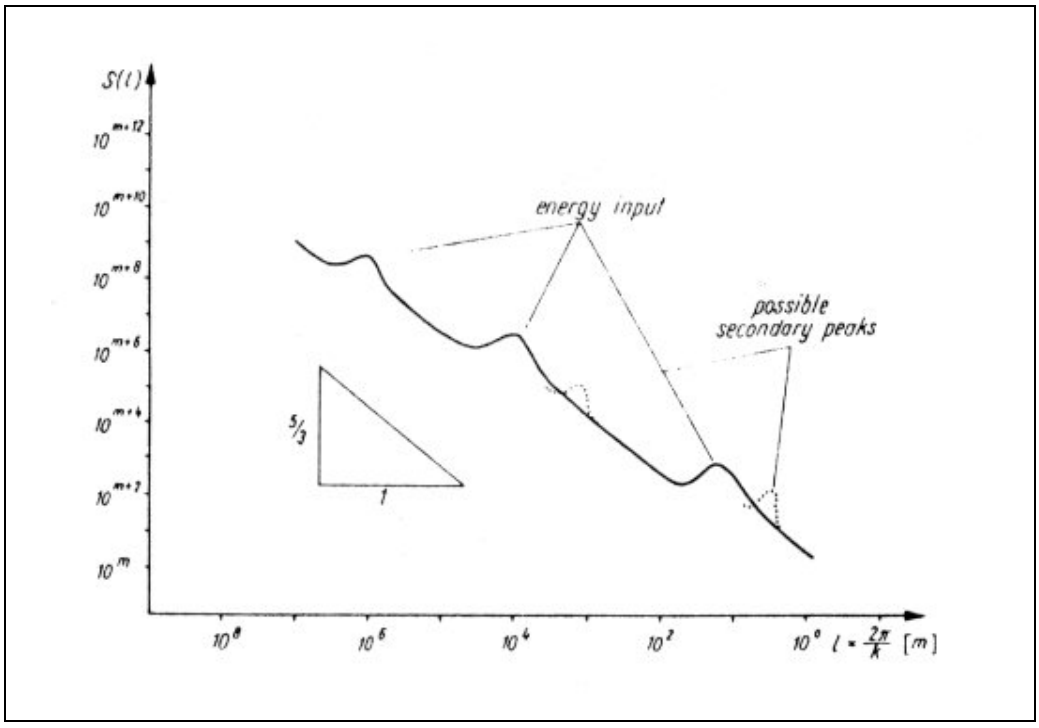

Figure 2.7: Typical turbulent energy spectrum (from Zeidler, 1976)

.

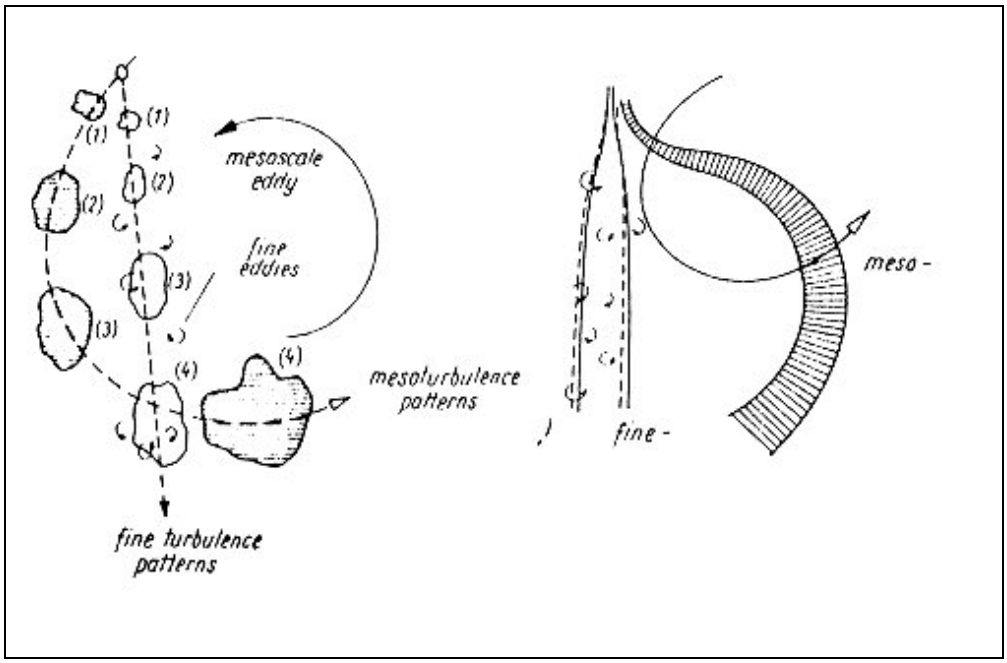

Figure 2.8: Different types of eddies in coastal waters, and their effect on mixing, from Zeidler (1976).

The mixing of a substance in nearshore areas is performed by a combination of small-scale turbulent diffusion and the large-scale variation of the mean velocity flux. In models that attempt to reproduce dispersion in coastal waters, it is possible to discriminate between small scale eddies and mesoscale eddies, which are related to different types of diffusion (fig. 2.8). The former eddies enhance dilution but do not break the nearly regular structure of a pollutant plume, whereas the latter tend to transport the whole of the plume, maintaining the overall concentration. Small scale turbulence can be included in the dispersion analysis using the semi-empirical theory of turbulence, based on a quasi-deterministic approach (Zeidler, 1976). On the other hand, mesoscale eddies are taken into account by using turbulence models, which are described in §2.3.1.1.

2.2.5 Tides. Tidal currents

Tide is the name given to the alternate rise and fall of the sea level with an average period of 12.4 hrs, due to the simultaneous action of the Moon's, Sun's and Earth's gravitational forces, the revolving of the Moon around the Earth, and of the Earth around the Sun. This rhythmic rise and fall of water is a characteristic feature of many coastal areas

2.2.5.1 Tides

Tidal oscillations are produced by the forces set up by the Earth/Sun and Earth/Moon pairs. Considering only the Earth/Moon pair, whereas the centripetal force that keeps an approximately constant separation between them as they revolve around the systems's centre of mass is the same all over the Earth's surface, the gravitational force exerted by the Moon is strongest on the side of the Earth closest to the Moon, and weakest on the opposite one. The difference in magnitude between both forces results in a residual force, the (locally) horizontal component of which is the tide-producing (tractive) force; the local magnitude variation of the resulting force due to the rotation of the Earth leads to the characteristic behaviour of the tides. In the particular case of the Earth/Moon

pair, the tractive forces are zero along a meridian perpendicular to the Earth-Moon axis, and at the farthest and nearest points from the Moon; they are maximal along meridians at 45º from this axis, being towards the Moon on the near side of the Earth, and away from it on the far side. A similar force pattern is set up be the Earth/Sun pair; the overall resulting force pattern, however, becomes complicated because the Sun and the Moon do not revolve in synchronism, their orbital trajectories are ellipses, rather than circles, and their orbital planes are generally offset.

The vertical differences between successive high and low waters, i.e., the tidal range, vary considerably from place to place, depending on the location, bottom topography and the coastal features. Measured tidal ranges vary from almost zero to about 15 m (in the Bay of Fundy, New Brunswick, Canada -Pond and Pickard, 1989-). Large tidal ranges are usually found in estuaries or rivers -due to the "funnelling effect" resulting from the tidal wave propagation in a narrower and shallower environment-, and in some bays -due to resonance, when the natural period of oscillation of the water in the bay is close to that of the astronomical tide (as occurs in the Bay of Fundy). Because of this complexity, the analysis and prediction of tides relies almost completely on the recording of water fall and rise as a function of time, and the subsequent use of mathematical procedures (harmonic analysis or response method) to deduce the expected tidal height for any future time.

The harmonic analysis consists in decomposing the tidal curve into simple harmonics (sine functions) of different periods, phases and amplitudes, projecting the individual constituents forward in time, and adding them up to determine the expected tidal height at the desired time. The individual constituents are divided into three classes according to their period: semi-diurnal (with $T_t \cong 12$ hrs), diurnal ($T_t \cong 24$ hrs) and long period (with T_t greater than one day, usually of about 2 weeks). Up to 65 constituents have been recognised as significant in some circumstances, such as describing tides in river estuaries.

The response method, also called Fourier method, consists in carrying out a Fourier spectral analysis on the tide records, regarding them as a time series, determining amplitudes and phases at equal frequency intervals. The advantage of this method is that it allows separation of the gravitational from the non-gravitational effects.

An alternative approach is to use numerical methods to solve the Laplace equations. Even though this method is simple in principle, it can become very complicated if real ocean shapes and bottom topography are to be included.

2.2.5.2 Tidal currents

Although the rise and fall of the water level is the most obvious effect, the primary tidal phenomena are the horizontal currents; so, the sea level variations at the coast are a consequence of the divergence or convergence occurring when tidal currents flow away from or towards the shore. The effects of tidal currents are twofold: on the one hand, they may cause large daily changes in the volume of water in a bay, and on the other hand they may promote vertical mixing, thus breaking down the stratification of the water column.

In the open waters of the continental shelf, or in shallow open seas, tidal currents are characterised by a changing speed, often never decreasing to zero, and a rotating direction, usually with a dominating semi-diurnal period. In narrow waterways, such as estuaries, the common tidal pattern is composed of a flood current in one direction as the tide rises, and an ebb current in the opposite direction while it falls. Typical values of tidal current speeds are given in Pond and Pickard (1989) as less than about 0.1 m/s away from the coast, but these authors point out that much higher

values are common in straits and passages, as in the Seymour Narrows (British Columbia, Canada), where tidal currents of up to 8 m/s have been measured.

Tidal waves can be considered as long waves with lengthwaves of hundreds of kilometres; when they propagate onto the continental shelf, they become influenced by shallow coastal waters. Because of the difference in water depth at high and low water, the tidal trough is retarded more than its crest, since frictional effects are larger. The usual description of tides in shallow waters is done using a system of depth-integrated equations (eqs. (2.106) and (2.107)), and the continuity equation as given by (2.108) - Massel, 1989-:

$$\frac{\partial u_t}{\partial t} + u_t \frac{\partial u_t}{\partial x} + v_t \frac{\partial u_t}{\partial y} - f u_t = -g \frac{\partial \bar{\eta}}{\partial x} - \frac{\tau_b^x}{\rho d} \tag{2.106}$$

$$\frac{\partial v_t}{\partial t} + u_t \frac{\partial v_t}{\partial x} + v_t \frac{\partial v_t}{\partial y} + f u_t = -g \frac{\partial \bar{\eta}}{\partial y} - \frac{\tau_b^y}{\rho d} \tag{2.107}$$

$$\frac{\partial \bar{\eta}}{\partial t} + \frac{\partial (u_t d)}{\partial x} + \frac{\partial (v_t d)}{\partial y} = 0 \tag{2.108}$$

where f is the Coriolis parameter (= $2\Omega_E \sin\phi_G$, with ϕ_G the latitude and Ω_E the earth's angular rate of rotation) and $d = h + \bar{\eta}$.

These equations evidence that the shallow water constituents of the tidal currents are described by non-linear terms in the equations of motion. Therefore, a solution of eqs. (2.106)-(2.108) must be based on the use of available numerical techniques (Massel, 1989). An estimation of the current velocities can be made, however, by making certain simplifying assumptions to linearise (2.106)-(2.108). By considering the tidal wave as a progressive wave travelling in a constant-depth wide channel, imposing small acceleration terms and a small tidal elevation $\bar{\eta}$ compared to the water depth h, and neglecting bottom stresses, the equations of motion can be expressed as

$$\frac{\partial u_t}{\partial t} = -g \frac{\partial \bar{\eta}}{\partial x} \tag{2.109}$$

$$f u_t = -g \frac{\partial \bar{\eta}}{\partial y} \tag{2.110}$$

$$h \frac{\partial u_t}{\partial x} = -\frac{\partial \bar{\eta}}{\partial t} \tag{2.111}$$

which, after some manipulation, lead to a solution of the type

$$\begin{aligned} \bar{\eta} &= a_t e^{-cy} \cos(kx - \omega t) \\ u_t &= \sqrt{\frac{g}{h}} a_t e^{-cy} \cos(kx - \omega t) \end{aligned} \tag{2.112}$$

where $c = f / \sqrt{gh}$ and a_t is the tidal amplitude. Equations (2.112) describe a Kelvin wave travelling in the x direction.

Other wave-like solutions to the governing equations of motion can be found by considering different assumptions (Massel, 1989).

2.2.6 Estuarine circulation

The water circulation in estuarine regions presents a fairly complex pattern due to a series of unique characteristics of these water bodies. Because of the constant inflow of freshwater from discharging rivers, the water mass in an estuary is formed by the coexistence of a fresh or brackish water, and a saline water which has intruded into the estuary from the ocean, leading to variations in salinity and temperature (and, therefore, in density) in the different parts of the estuary. The density effects, the relative amount of freshwater inflow, and the relationship of the estuary or bay to the open ocean all result in a complicated two-layered flow in some regions of tidal water bodies.

The main feature of the estuarine flow pattern is the superimposition of a fresh to brackish water surface layer, and a layer of more saline and cold water, separated by a clearly marked pycnocline; the severe vertical stratification has a significant effect on sediment and dissolved oxygen transport, and on the cycling of nutrients. An arrested salt wedge is usually found extending a certain distance up the river from the mouth, stationary except for internal circulation. The thickness of each layer depends on a number of factors, amongst which the most important is the amount of freshwater discharged by the river. The lighter surface water flows seaward, whereas the denser bottom water flow is in the opposite direction.

Additionally, the landward transport of bottom water and the seaward transport of freshwater generate vertical velocities in the estuary water, which result in the appearance of a convergence zone in the vicinity of the limit of saltwater intrusion. The suspended solids in the estuary are transported downstream in the surface waters, settle into the bottom waters, and then may be recycled upstream to the convergence area. In that vicinity, a “turbidity maximum” may occur. This is a region of the estuary where suspended solids concentrations are high because of the complex horizontal and vertical velocities and the local resuspension of sediments from the bed. The transport of particulate and dissolved nutrients can also result in nutrient intensification or “trapping” in estuaries.

Amongst the factors which influence the estuarine water circulation, the following also play a major role in the dispersion of substances in estuaries:

a) Wind, which may or may not be the main driving agent in an estuary, depending largely on the physical characteristics of the basin; whereas in shallow, wide estuaries the current induced by wind stresses may be important, in long, narrow estuaries the flow will be predominantly tidal (Fischer *et al.*, 1979).

b) Tides, which affect the water circulation in two ways. On one hand, the friction of the tidal flow on the channel bottom generates turbulent fluctuations of the water velocity; on the other, the interaction between the tidal wave and the physical configuration of the estuary generates larger scale motions, such as the “tidal pumping”. This is the process by which a preferential direction is set up for the residual circulation (Beer, 1997), i.e., the net steady circulation superimposed on the periodic tidal flow. This residual flow is caused by the Coriolis deflection in large estuaries (in which the width exceeds the product of the inertial period and the tidal current speed), inducing a net counter-clockwise circulation in the northern hemisphere, and by the interaction of the tidal flow with the irregular bathymetry of most estuaries.

Both effects play major roles in the diffusion and overall transport of substances in estuarine waters.

c) Rivers. If the freshwater inflow into an estuary is high compared to the tidal currents, a marked salinity difference can occur between the upper and lower layers, because the turbulent energy from the tidal flow is insufficient to significantly mix the incoming saline water with the waters of riverine origin. The river itself is a source of buoyancy, and thus density currents may be of importance, tending to bring the (sloping) isohalines to the horizontal. This baroclinic circulation appears even in vertically well-mixed estuaries, driven by the longitudinal density gradients.

The relation between velocity components, pressure and salinity at any point (*x*, *y*, *z*) in a tidal estuary can only be described with the use of a three-dimensional formulation due to the complexity of the problem. The governing equations are the momentum equations in the two horizontal directions (equation (2.13), with i=1,2) and the continuity equation for water -equation (2.12)-, plus a continuity equation for salt -equivalent to a transport equation in the form (2.14)-.

A simplified model (two-layer model) which is frequently used consists in assuming that there is no mixing between the two layers (i.e., the respective densities remain constant). Making further assumptions such as a constant estuary width, a hydrostatic pressure distribution and an approximately uniform velocity distribution within each layer, the following continuity and motion equations can be derived (Abraham, 1976):

$$\begin{aligned} \frac{\partial h_1}{\partial t} + \frac{\partial h_1 u_1}{\partial x} &= 0 \\ \frac{\partial h_2}{\partial t} + \frac{\partial h_2 u_2}{\partial x} &= 0 \end{aligned} \qquad (2.113)$$

$$\begin{aligned} &\frac{\partial u_1}{\partial t} + u_1 \frac{\partial u_1}{\partial x} + g\frac{\partial h_1}{\partial x} + g\frac{\partial h_2}{\partial x} - gi + \frac{\tau_{ei}^x}{\rho_1 h_1} = 0 \\ &\frac{\partial u_2}{\partial t} + u_2 \frac{\partial u_2}{\partial x} + \frac{\rho_1}{\rho_2} g\frac{\partial h_1}{\partial x} + g\frac{\partial h_2}{\partial x} - gi + \frac{\tau_{ei}^x - \tau_{eb}^x}{\rho_2 h_2} = 0 \end{aligned} \qquad (2.114)$$

where h_j, u_j, and ρ_j (j=1, 2) are the thickness, velocity and density of each layer, i is the bottom slope, τ_{ei}^x is the shear stress at the interface, and τ_{eb}^x is the shear-stress at the bottom.

A measure of the estuarine stratification is given by the so-called "estuarine Richardson number" Ri_e, defined as

$$Ri_e = \left(\frac{\Delta\rho}{\rho}\right)\frac{gQ_R}{W\,u_{t,rms}^3} \qquad (2.115)$$

where $u_{t,rms}$ is the rms tidal velocity, Q_R is the fresh water discharge rate, and W is the channel width. The number Ri_e expresses the ratio of the input of buoyancy due to fresh water per unit width of channel to the mixing power available from the tide. If Ri_e is very large, the estuary is expected to be strongly stratified, and the flow will be dominated by density currents; if Ri_e is very small, the density effects may be neglected, and the estuary will be well mixed. The transition from a well mixed to a strongly stratified estuary appears to be in the range $0.08 < Ri_e < 0.8$ (Fischer *et al.*, 1979).

The important phenomena in the setting of salt wedges in estuarine rivers are the tidal movement, the effect of density differences on velocity distribution, through the pressure gradient and the distribution of shear stress over the depth, and the effect of mixing on the distance the salt intrudes (Abraham, 1976). In addition, salt intrusion is also affected by exchange currents between the main channel and lateral branches or harbours, and by the vertical mixing and advective salt transport, which limits the distance the salt can intrude inland.

2.3 MIXING IN COASTAL WATERS AND ESTUARIES

2.3.1 Turbulent diffusion and dispersion. Mixing coefficients

When matter is discharged into a non-stagnant environment, its concentration distribution is distorted by two major types of transport: bulk motion and turbulent motion. The discharged substance is carried away from the source by the general water circulation (bulk motion), and it is simultaneously spread out in the longitudinal and lateral directions by the diffusive effects of turbulent motion.

Moreover, lateral diffusion will move parcels of matter into regions with different bulk velocities, leading to an acceleration of the material in the direction of the flow, and to an additional spreading mechanism. The scattering of particles, or a cloud of contaminant substance, by the combined effects of lateral velocity shear and turbulent diffusion is called dispersion (Gallagher and Hobbs, 1978).

The total flux of mass in a unit volume shows a contribution due to turbulent diffusion, plus a contribution from the flux of material transported by the bulk motion. Therefore,

$$(\text{total flux of mass}) = \sum_i u_i C + D_i \frac{\partial C}{\partial x_i} \qquad (2.116)$$

By summing up all the fluxes, and taking derivatives with respect to the spatial coordinates, a three-dimensional balance equation for mass can be obtained and, theoretically, solved. This procedure, however, is seldom followed (Gallagher and Hobbs, 1978), and the usual practice is to average equation (2.116) over one or more dimensions to reduce the complexity of the problem. A side effect of this simplification is the introduction of an effective dispersion coefficient K_i, representing the combined effects of shear stress and turbulent diffusion, as a substitute of the turbulent diffusivity D_i .

A simple example appears by averaging the transport equation in the vertical and lateral directions, thus obtaining a 1D equation for longitudinal transport only:

$$\frac{\partial(A\overline{C})}{\partial t} = -\frac{\partial}{\partial x}(A\overline{u}\overline{C}) + \frac{\partial}{\partial x}(AK_x \frac{\partial \overline{C}}{\partial x}) \qquad (2.117)$$

in which $\overline{C}$ and $\overline{u}$ are concentration and longitudinal velocity averaged over the cross-sectional area *A(x,t)*. Here, the deviations from the mean velocity $\overline{u}$ ($u' = u - \overline{u}$) are included in a dispersive term, formally equal to a diffusive term, instead of appearing in the advective part of the equation.

In general, the dispersion coefficient K_x can be expressed as a function of the velocity fluctuations and the turbulent diffusion coefficients

$$K_x = K_x (u-\bar{u}, D_x, D_y, D_z) \tag{2.118}$$

but it is convenient to split it into components

$$K_x = \overline{D_x} + K_{xy} + K_{xz} \tag{2.119}$$

where $\overline{D_x}$ is the cross-sectional mean longitudinal diffusivity and K_{xy} and K_{xz} are the longitudinal dispersion coefficients due to lateral and vertical shear, respectively.

It appears clear that, in order to make a quantitative estimate of the dispersion suffered by a substance discharged into any waterbody, a quantitative knowledge of the bulk water motion and some measure of its strength is required.

2.3.1.1 Turbulent diffusion coefficients. Turbulence models

The turbulent diffusion is that process generated by the fluctuating nature of the flow, which loses its laminar characteristics when the Reynolds number, defined as the ratio between the inertial and the viscous forces, becomes greater than a critical value, typically about 2000 (Tennekes and Lumley, 1987). In the state of turbulent flow, each fluid element has a velocity that can be thought of as a mean value with random fluctuations about it. It is worth noting that this separation into two components can be applied to any property that characterises a fluid element, such as pressure, concentration, etc. The turbulent transport of mass, heat or momentum is related to the correlations between fluctuations, and is described by means of the turbulent diffusion coefficients.

These fluctuations, or turbulent components of the velocity, define a range of movement scales in which the turbulent flow takes place; the biggest are given by the physical properties of the water body and the flow, whereas the smaller ones (Kolmogorov scales) are related to turbulent kinetic energy dissipation (§2.2.4).

The most general form of mass conservation in a control volume subject to advective and diffusive flux across its boundaries is

$$\frac{\partial C}{\partial t} + \mathbf{u}\nabla C = D_m \nabla^2 C \tag{2.120}$$

which incorporates an assumption of incompressible ambient fluid and uses Fick's first law of simple proportionality between the diffusive contaminant flux and the concentration gradient, and where D_m is a property of the contaminant and the ambient fluid only, but not of the flow.

Equation (2.120), however, is not useful because it requires the knowledge of the velocity vector $\boldsymbol{u}(x,y,z,t)$ and concentration field $C(x,y,z)$ with sufficient time and space precision to resolve the details of random turbulent fluctuations. Since this is not possible, equation (2.116) must be replaced by some average description of the dispersion process, as explained in §2.1.2:

$$\frac{\partial \overline{C}}{\partial t} + \overline{\mathbf{u}} \nabla \overline{C} = D_m \left(\frac{\partial^2 \overline{C}}{\partial x^2} + \frac{\partial^2 \overline{C}}{\partial y^2} + \frac{\partial^2 \overline{C}}{\partial z^2} \right) - \frac{\partial}{\partial x}\left(\overline{u'c'}\right) - \frac{\partial}{\partial y}\left(\overline{v'c'}\right) - \frac{\partial}{\partial z}\left(\overline{w'c'}\right) \qquad (2.121)$$

where the last three terms represent the isolation of contaminant transport due to turbulent advection.

Taylor's theory (1921) states that the variance of a cloud of particles released into a homogeneous and stationary turbulent flow increases linearly with time at a rate given by $2\,\overline{\overline{u'^2}}\,L_{tx}$,, where $\overline{\overline{u'^2}}$ is the mean-square velocity fluctuations and L_{tx} is the Lagrangian integral timescale of turbulence, given by

$$L_{tx} = \int_0^\infty R_{u'}(\tau)\,d\tau = \int_0^\infty \frac{\overline{u'(t)u'(t+\tau)}}{\overline{\overline{u'^2}}}\,d\tau \qquad (2.122)$$

with $R_{u'}(\tau)$ the Lagrangian correlation coefficient for successive particle displacements, and where the double overbar denotes an ensemble average. Moreover, another characteristic feature of gradient diffusion processes is that the variance of the distribution increases linearly with time (Fischer *et al.*, 1979). So, the terms corresponding to turbulent transport in equation (2.121) can also be written as a gradient diffusion process,

$$D\frac{\partial \overline{C}}{\partial x} = -\overline{u'c'} \qquad (2.123)$$

where D is a diffusion coefficient. Zeidler (1976) called D an "effective" diffusion coefficient, arguing that it is not coupled with random turbulent fluctuations of the velocity and concentration fields, but rather with their interaction. Since molecular diffusion is independent of turbulent motion, equation (2.121) can be written

$$\frac{\partial \overline{C}}{\partial t} + \overline{u} \nabla \overline{C} = \frac{\partial}{\partial x}\left(D_x \frac{\partial \overline{C}}{\partial x} \right) + \frac{\partial}{\partial y}\left(D_y \frac{\partial \overline{C}}{\partial y} \right) + \frac{\partial}{\partial z}\left(D_z \frac{\partial \overline{C}}{\partial z} \right) \qquad (2.124)$$

where the diffusivities are in the form $D_i = D_m - \dfrac{\overline{u_i'c'}}{\partial \overline{C}/\partial x_i}$.

It is important to note that the presence of non-zero correlation terms involving the fluctuation components of the different variables is a consequence of the decomposition of physical variables and the subsequent time averaging of the Navier-Stokes equation (equation 2.3). Even though the number of these unknown correlation terms may be reduced by assuming certain symmetries, there are always some that remain in the equations, and must be treated somehow in order to find a correct solution to the set of equations (2.12-2.14). This is referred to as the "turbulence closure problem", and it is generally coped with by introducing some type of turbulence model to close the equation system.

The use of turbulence models to overcome the closure problem relies on the approximation of correlations of a certain order in terms of mean-flow quantities, such as velocity gradients, and/or lower-order correlations. However, whereas in principle the fundamental equations describe all flows,

the various closure schemes do introduce a certain loss of generality, depending upon the quality of the model.

A widespread understanding of turbulence is that it can be viewed as a large number of intermingled eddies, each with different velocity and size. From this perspective, a new concept which is basic in turbulence studies can be defined. In analogy with molecular motion, turbulent eddies may be thought of as lumps of fluid which collide and exchange momentum, generating turbulent stresses. Boussinesq proposed that, in a similar way to viscous stresses, the former could be assumed to be proportional to the mean flow gradients:

$$-\overline{u_i' u_j'} = \nu_t \left(\frac{\partial \overline{u}_i}{\partial x_j} + \frac{\partial \overline{u}_j}{\partial x_i} \right) - \frac{2}{3} k \delta_{ij} \tag{2.125}$$

where the proportionality constant ν_t is the turbulent or eddy viscosity, which depends not on the fluid but on the state of turbulence in the flow, and the decomposition of variables given in (2.11) has been used. By introducing the eddy viscosity, the modelling of turbulence is reduced to determining the distribution of ν_t. The last term in equation (2.125) is necessary to impose that the sum of all normal stresses (i.e., $i=j$) is equal to twice the kinetic energy k. Since it represents a pressure, when introducing equation (2.125) in the momentum equation, this term can be included in the pressure-gradient term, substituting the unknown static pressure p by $p' = p + 2/3k$.

Similarly, the turbulent transport of a scalar quantity C is often assumed to be proportional to the gradient of C:

$$-\overline{u_i' c'} = D \frac{\partial C}{\partial x_j} \tag{2.126}$$

where D is the eddy-diffusivity, which also depends on the state of turbulence, and which is related to the eddy viscosity through the turbulent Prandtl or Schmidt number

$$\sigma_t = \frac{\nu_t}{D} \tag{2.127}$$

A description of the velocity fluctuations (or ν_t) can be quantitatively given by the turbulence spectrum, and the latter can be described in a simple manner by two parameters: a velocity-scale, related to the amplitude of the most energetic eddies, and a lengthscale which sets the position of the large eddies in the wave-number space. One, or both, of these parameters form the basis of the turbulence models described below.

a) Zero-equation models

In the lower-order models, no transport equations for turbulent quantities are considered, and the turbulence is described by means of the eddy viscosity, which is assumed to be either a constant throughout the whole flow field or a function of the mean flow velocity (mixing length models). In the former case, the eddy viscosity is specified from experiments, trial-error procedures, or empirical formulae. Since they do not account for local turbulence changes they cannot be considered proper turbulence models.

a.1) Constant eddy viscosity

In large water bodies, many hydrodynamic calculation methods use a constant value of the eddy viscosity for the whole flow field. This simple approach is possible because in some cases the turbulence

terms in the momentum equations are not important, so the accuracy of the model has no relevant influence. On the other hand, on the occasions when the turbulent terms do become important the hydrodynamic model is usually too coarse to describe the turbulent behaviour of the flow correctly.

The preceding argument cannot be extended to the transport equations, since their turbulent terms are always important. A constant-diffusivity model can only be applied where the diffusivity presents slow variations, as in the farfield, and even then the results are relatively crude. In the nearfield, the turbulence is governed by local disturbances such as discharges, and the diffusivity can never be taken as a constant.

The assumption of a constant eddy viscosity/diffusivity imposes no condition on the isotropy of the turbulence field. In fact, for numerical reasons, different values of ν_t for the horizontal (ν_H) and vertical (ν_V) momentum transfer are generally accepted, where ν_H is usually taken to be greater than ν_V. In this case, the diffusivities are usually related to the shear velocity u_*, accepting that turbulence is due mainly to the bottom roughness. The generally accepted values of the diffusion coefficients are given in table 2.1, in which u_* stands for the bottom shear velocity, and κ is the von Karman constant (0.41).

	Coefficient	Generally accepted value	Comments
Molecular diffusion	D_m	$\approx 10^{-9}$ m^2/s	It depends on the fluid and the pollutant.
3 dimensional boundary-free turbulent diffusion	D_x D_y D_z	?	Determined from measurements or turbulence models.
3 dimensional turbulent diffusion in shear-flows	D_x D_y D_z	$\kappa u_* h / 6$ $0.23\, u_* h$ $\kappa u_* h / 6$	Reynolds analogy. Elder (1959) assumed D_x=D_z.
Depth-averaged dispersion, plane flow	K_x $\overline{D_y}$	$5.93\, u_* h$ $0.23\, u_* h$	A logarithmic velocity profile is assumed Elder (1959).
Depth-averaged flow in channel	K_x K_y	$5.93\, u_* h$ $\overline{D_y}$ + ?	The effects of secondary currents in K_y are difficult to quantify.
1D cross-sectional average dispersion, turbulent pipe flow	K_x	$10.1 u_* r$	
1D cross-sectional average dispersion, turbulent river flow	K_x	$-\frac{1}{A}\int$	Strongly dependent on channel geometry and flow patterns.

Table 2.1: Diffusion coefficients for different types of flow (from Holly, 1985).

The solution of a numerical calculation for large water bodies with a constant value for the diffusivity corresponds to the use of a D which is only in part due to turbulence, but includes also additional non-turbulent processes, such as numerical diffusion, sub-grid scale convective motion, or dispersion (for depth-averaged calculations). The choice of a suitable D is then not a turbulence-model problem, but rather a question of numerical calibration.

a.2) Mixing-length models

These models describe the spatial distribution of the eddy viscosity, and can therefore be considered the first real turbulence models. Based on the Prandtl mixing-length hypothesis, they assume that ν_t is proportional to a velocity scale and a mixing length l_m; this velocity scale is postulated to be equal to the mean velocity gradient multiplied by l_m, so that the eddy viscosity can be expressed as

$$\nu_t = l_m^2 \left| \frac{\partial \bar{u}}{\partial y} \right| \tag{2.128}$$

in two-dimensional shear layer flows.

For simple flows, l_m can be specified in many situations from simple empirical formulae; in free layers, for instance, it is usually assumed to be proportional to the local layer width.

The Prandtl mixing-length hypothesis for general flows may be written as

$$\nu_t = l_m^2 \left[\left(\frac{\partial \bar{u}_i}{\partial x_j} + \frac{\partial \bar{u}_j}{\partial x_i} \right) \frac{\partial \bar{u}_i}{\partial x_j} \right] \tag{2.129}$$

but this expression is rarely used due to the difficulty of specifying l_m in complex situations.

The mixing-length models are not suitable when convection or diffusion of turbulence is important, since they do not account for the transport of turbulence parameters. Additionally, these models are of little use in complex flows because of the difficulties in computing l_m, as mentioned above.

b) One-equation models

To overcome the problems appearing in mixing-length models, other models were developed to account for the transport of turbulent quantities; this was done by introducing and solving differential transport equations for them. The one-equation models drop the direct relationship between velocity gradients and the fluctuating velocity scale, and determine the latter from a transport equation.

In the eddy-viscosity models, the velocity fluctuations can be characterised by the kinetic energy of the turbulent motion, per unit mass (or k):

$$k = \frac{1}{2} \left(\overline{u'_i u'_i} \right)^{1/2} \tag{2.130}$$

since it is a measure of the intensity of the turbulence fluctuations in the three directions. The eddy-viscosity can then be expressed in the form of the Kolmogorov-Prandtl equation (Rodi, 1984)

$$\nu_t = c'_\mu \sqrt{k} L_t \tag{2.131}$$

with c'_μ being an empirical constant and L_t a large-scale turbulence lengthscale, which is as difficult to determine as l_m was in the zero-equation models. The distribution of k can be determined by solving its

exact transport equation, which is derived from the Navier-Stokes equation. For high Reynolds numbers, it reads

$$\frac{\partial k}{\partial t}+\bar{u}_i\frac{\partial k}{\partial x_i}=-\frac{\partial}{\partial x_i}\left[\overline{u'_i\left(\frac{u'_j u'_j}{2}+\frac{p}{\rho}\right)}\right]-\overline{u'_i u'_j}\frac{\partial \bar{u}_i}{\partial x_j}-\beta g_i\overline{u'_i c'}-\nu\overline{\frac{\partial u'_i}{\partial x_j}\frac{\partial u'_i}{\partial x_j}} \qquad (2.132)$$

where the terms on the right-hand side represent the diffusive transport, the production of k by shear (Reynolds stresses and mean velocity gradients), the production/destruction of k due to buoyancy fluxes, and the dissipation of k into heat by viscous action, respectively. In equation (2.132), ν is the fluid viscosity and β is the volumetric expansion coefficient of water.

The terms in (2.132) involving new unknown correlations are modelled as follows: the diffusion flux of k is taken as proportional to the gradient of the kinetic energy,

$$\overline{-u'_i\left(\frac{u'_j u'_j}{2}+\frac{p}{\rho}\right)}=\frac{\nu_t}{\sigma_k}\frac{\partial k}{\partial x_i} \qquad (2.133)$$

whereas the viscous dissipation ε is modelled as

$$\varepsilon=\nu\overline{\frac{\partial u'_i}{\partial x_j}\frac{\partial u'_i}{\partial x_j}}=c_D\frac{k^{3/2}}{L_t} \qquad (2.134)$$

where σ_k and c_D are empirical constants. Substitution of all the correlation terms in (2.132) yields

$$\frac{\partial k}{\partial t}+\bar{u}_i\frac{\partial k}{\partial x_i}=\frac{\partial}{\partial x_i}\left(\frac{\nu_t}{\sigma_k}\frac{\partial k}{\partial x_i}\right)+\nu_t\left(\frac{\partial \bar{u}_i}{\partial x_j}+\frac{\partial \bar{u}_j}{\partial x_i}\right)\frac{\partial \bar{u}_i}{\partial x_j}+\beta g_i\frac{\nu_t}{\sigma_t}\frac{\partial c'}{\partial x_i}-c_D\frac{k^{3/2}}{L_t} \qquad (2.135)$$

which closes the system of equations. Reasonable values for the coefficients σ_k and $c_D \cdot c'_\mu$ seem to be 1 and 0.08, respectively (Launder and Spalding, 1972); the product $c_D \cdot c'_\mu$, rather than the individual values of the constants, is required because the solution to equation (2.135) is substituted into equation (2.131), and only $c_D \cdot c'_\mu$ appears.

The advantages of one-equation models over zero-equation models lay in the fact that the former include the effects of convective and diffusive turbulence transport and are thus useful when this transport is relevant. However, due to the complexity in specifying the lengthscale distribution, these models are mainly restricted to shear-layer flows.

c) Two-equation models

A further refinement is achieved in turbulence models by considering the transport of the lengthscale L_t. The processes that influence L_t are convection, dissipation, and vortex stretching. The use of a lengthscale transport equation is stimulated by the difficulty in finding generally valid empirical formulae for calculating L_t in a direct manner.

The dependent variable in the lengthscale equation can be any combination of the form $Z=k^m L_t^n$, since the value of the kinetic energy is known from solving the k-equation (2.135). The general form of this equation, for non-buoyant flows, is

$$\frac{\partial Z}{\partial t}+\bar{u}_i\frac{\partial Z}{\partial x_i}=\frac{\partial}{\partial x_i}\left(\frac{\sqrt{k}L_t}{\sigma_Z}\frac{\partial Z}{\partial x_i}\right)+c_{Z1}\frac{Z}{k}\left(-\overline{u'_i u'_j}\frac{\partial \bar{u}_i}{\partial x_j}\right)-c_{Z2}Z\frac{\sqrt{k}}{L_t}+Q_t \qquad (2.136)$$

where σ_z, c_{z1} and c_{z2} are empirical constants and Q_t is a "source" term which depends on the choice of Z. This source term is important in flows near walls for all choices of Z except for $Z=\varepsilon$ ($\sim k^{3/2}/L_t$) and it is for this reason that the so-called ε-equation has become the most widely used lengthscale equation in turbulence modelling.

The relationship between the two model variables and the eddy viscosity (analogue to the Kolmogorov-Prandtl equation) is found from dimensional analysis to be

$$\nu_t=c_\mu\frac{k^2}{\varepsilon} \qquad (2.137)$$

For high Reynolds numbers, where the turbulence tends to be isotropic, the following ε-equation is proposed

$$\frac{\partial \varepsilon}{\partial t}+\bar{u}_i\frac{\partial \varepsilon}{\partial x_i}=\frac{\partial}{\partial x_i}\left(\frac{\nu_t}{\sigma_\varepsilon}\frac{\partial \varepsilon}{\partial x_i}\right)+c_{1\varepsilon}\frac{\varepsilon}{k}\left(-\overline{u'_i u'_j}\frac{\partial \bar{u}_i}{\partial x_j}-c_{3\varepsilon}\beta g_i\overline{u'_i c'}\right)-c_{2\varepsilon}\frac{\varepsilon^2}{k} \qquad (2.138)$$

with σ_ε, $c_{1\varepsilon}$, $c_{2\varepsilon}$ and $c_{3\varepsilon}$ empirical constants.

Equations (2.137) and (2.138), together with the k-equation (2.135), form the basis of the k-ε model, which yields a purely local description of turbulence (Rodi, 1984). The values of the constants in the model are determined from experiments. Whereas there seems to be some controversy regarding the value of $c_{3\varepsilon}$ (Rodi, 1984), the other constants are widely accepted to be those given in table 2.2:

c_μ	$c_{1\varepsilon}$	$c_{2\varepsilon}$	σ_k	σ_ε
0.09	1.44	1.92	1.0	1.3

Table 2.2: Values of the constants in the k-ε model, as recommended by Launder and Spalding (1974).

d) Higher-order models

All of the previous models assumed that it is possible to relate the individual Reynolds's stresses to a single velocity scale which, in turn, characterises the local state of turbulence. Although it is frequent to find this situation in real flows, often the transport of the individual stresses is not properly accounted for, since the development of the turbulent fluctuations and their transport is different for each component, and in each direction. To allow for the development of the individual stresses, and to account for their transport, several models have been developed which employ transport equations for the stresses $\overline{u'_i u'_j}$ and the turbulent heat or mass fluctuations $\overline{u'_i c'}$. These equations, together with a two-equation model (e.g., k-ε), are usually referred to as second-order, or higher-order, closure models.

d.1) Reynolds's stress models

Launder *et al.* (1975) proposed substituting the exact transport equation for turbulent correlations with the following expression,

$$\frac{\partial \overline{u'_i u'_j}}{\partial t} + u_l \frac{\partial \overline{u'_i u'_j}}{\partial x_l} = c_S \frac{\partial}{\partial x_l}\left(\frac{k}{\varepsilon} \frac{\partial \overline{u'_i u'_j}}{\partial x_k} \right) - \varepsilon_{ij} - P_{ij} - G_{ij} - \pi_{ij,1} - \pi_{ij,2} - \pi_{ij,3} \tag{2.139}$$

in which the two terms on the left hand side represent the temporal variation and the advective transport of the correlations, the first term on the right accounts for the diffusion, the following term represents the dissipation,

$$\varepsilon_{ij} = \frac{2}{3}\delta_{ij}\varepsilon \tag{2.140}$$

P_{ij} and G_{ij} represent the production due to stresses and buoyancy, respectively,

$$P_{ij} = \overline{u'_i u'_l} \frac{\partial u_j}{\partial x_l} + \overline{u'_j u'_l} \frac{\partial u_i}{\partial x_l} \tag{2.141}$$

$$G_{ij} = \beta\left(g_i \overline{u'_j c'} + g_j \overline{u'_i c'} \right) \tag{2.142}$$

and the last three terms are the contribution to the turbulent momentum flux due to pressure strain:

$$\pi_{ij,1} = c_1 \left(\overline{u'_i u'_j} \frac{\varepsilon}{k} - \varepsilon_{ij} \right) \tag{2.143}$$

$$\pi_{ij,2} = \alpha\left(P_{ij} - \frac{2}{3}\delta_{ij} p \right) + \beta'\left(D_{ij} - \frac{2}{3}\delta_{ij} p \right) + \gamma k \left(\frac{\partial u_i}{\partial x_j} + \frac{\partial u_j}{\partial x_i} \right) \tag{2.144}$$

$$\pi_{ij,3} = c_3 \left(G_{ij} - \frac{2}{3}\delta_{ij} G \right) \tag{2.145}$$

where

$$D_{ij} = -\overline{u'_i u'_l} \frac{\partial u_l}{\partial x_j} - \overline{u'_j u'_l} \frac{\partial u_l}{\partial x_i} \tag{2.146}$$

$$\alpha = \frac{c_2 + 8}{11}; \qquad \beta' = \frac{8c_2 - 2}{11}; \qquad \gamma = \frac{30c_2 - 2}{55} \tag{2.147}$$

The transport equation for the scalar fluctuations is taken as (Gibson and Launder, 1978),

$$\begin{aligned} \frac{\partial \overline{u'_i c'}}{\partial t} + u_l \frac{\partial \overline{u'_i c'}}{\partial x_l} = c_{Sc'} \frac{\partial}{\partial x_l}\left(T_K \overline{u'_k u'_l} \frac{\partial \overline{u'_i c'}}{\partial x_k} \right) - \beta g_i \overline{c'^2}\left(1 + c_{3c'}\right) - \overline{u'_i u'_j} \frac{\partial C}{\partial x_j} - \\ - \overline{u'_i c'} \frac{\partial u_i}{\partial x_j} - \frac{c_{1c'}}{T_K} \overline{u'_i c'} - c_{2c'} \overline{u'_l c'} \frac{\partial u_i}{\partial x_l} \end{aligned} \tag{2.148}$$

In this equation, the first term on the right represents diffusion, followed by a term which includes the contribution of buoyancy effects; the following two terms take into account the mean-field production, and the last terms represent the pressure stresses; T_K is a turbulent correlation timescale.

The higher-order correlation appearing in equation (2.148) requires an additional transport equation,

$$\frac{\partial \overline{c'^2}}{\partial t} + u_l \frac{\partial \overline{c'^2}}{\partial x_l} = c_{c'} \frac{\partial}{\partial x_l}\left(\overline{u'_k u'_l} \frac{\partial \overline{c'^2}}{\partial x_k} \right) - P_{c'} - \varepsilon_{c'} \qquad (2.149)$$

with

$$P_{c'} = \overline{2u'_l c'} \frac{\partial C}{\partial x_j}; \qquad \varepsilon_{c'} = \frac{1}{Q_t} \frac{\overline{c'^2}}{k} \varepsilon \qquad (2.150)$$

Different values for the empirical constants which appear in equations (2.139) to (2.150) have been given by several authors, all of them yielding results which are physically realistic. The values proposed by Gibson and Launder (1978) are:

c_S	c_1	c_3	c_{1c}	c_{2c}	$c_{3c'}$	Q_t	α
0.8	1.5	0.5	3.0	0.33	0.33	0.33	0.6

d.2) Algebraic stress/flux models

In addition to the continuity, momentum and scalar flux equations, the models above require the solution to a minimum of 10 differential equations in general flows, corresponding to the transport of the 6 components of the Reynolds's stresses, plus the transport of the three components of the scalar flux, plus the equation for the scalar fluctuations. To avoid the enormous computational effort that this number of equations implies, several simplifications have been introduced to reduce (2.139) and (2.148) to equivalent algebraic expressions.

The simplest model is to assume that the gradients of the dependent variables (appearing only in the rate of change, convection and diffusion terms) can be neglected. A more accepted approach is to consider that the transport of turbulent correlations is proportional to the transport of the kinetic energy *k* (Rodi, 1976), so

$$\overline{u'_i u'_j} = k \left\{ \frac{\frac{2}{3}\delta_{ij} + \frac{(1-\alpha)}{\varepsilon}\left(P_{ij} - \frac{2}{3}\delta_{ij} p \right) + \frac{(1-c_3)}{\varepsilon}\left(G_{ij} - \frac{2}{3}\delta_{ij} G \right)}{c_1 + \frac{P+G}{\varepsilon} - 1} \right\} \qquad (2.151)$$

This equation can be used only in connection with a *k*-equation, such as equation (2.135), since it only allows the determination of the individual stresses, but not of *k*.

For the scalar flux, Gibson and Launder (1976) proposed the following algebraic expression, after simplifying (2.148),

$$\overline{u'_i c'} = \frac{\frac{k}{\varepsilon_c}\left\{\overline{u'_i u'_l}\frac{\partial C}{\partial x_l} + (1+c_{2c})\left(\overline{u'_l c'}\frac{\partial u_i}{\partial x_l} + \beta g_i \overline{c'^2}\right)\right\}}{c_1 + \frac{1}{2}\left(\frac{P+G}{\varepsilon} - 1\right)} \tag{2.152}$$

using (2.149) as the equation for turbulent scalar correlations, after neglecting the first three terms:

$$\overline{c'^2} = -2Q_t \frac{k}{\varepsilon_c}\overline{u'_i c'}\frac{\partial C}{\partial x_j} \tag{2.153}$$

Further simplifications to the transport equations may be introduced when the flows under consideration evolve so slowly that the rate of change and the transport of turbulent stresses and fluxes can be justifiably neglected altogether to first approximation. This is the case of thin shear layers, for which the algebraic expressions are (2.151) and (2.152), but with the factor $(P + G)/\varepsilon$-1 deleted from the denominator.

2.3.1.2 Dispersion coefficients

In laminar and turbulent flows, changes in velocity at different locations lead to the appearance of stresses which contribute to the spreading of pollutant clouds. The dispersive effects due to these mean flow gradients (or shear flow dispersion) are described using dispersion coefficients.

As with turbulent diffusion coefficients, and because of the disparity of lengthscales involved, the dispersive effects are commonly decomposed into two uncoupled parts, one accounting for dispersion in the horizontal plane *xy* and quantified by a horizontal coefficient K_H, and one describing dispersion in the vertical direction (K_V). In flows for which a preferred direction exists, as that defined by current lines, a longitudinal dispersion coefficient (K_L) and a lateral coefficient (K_T) can be further defined; the former corresponds to horizontal dispersion parallel to the direction of the current, while the latter represents horizontal dispersion in a direction normal to the current lines. When the turbulence can be considered horizontally isotropic, as in the surf zone after wave breaking, a single horizontal coefficient K_H suffices.

The relationship between K_L, K_T and K_x, K_y, taking δ as the angle between the current line and the *x*-axis, is

$$\begin{pmatrix} K_x & K_{xy} \\ K_{yx} & K_y \end{pmatrix} = \begin{pmatrix} \cos\delta & \sin\delta \\ -\sin\delta & \cos\delta \end{pmatrix}\begin{pmatrix} K_L & 0 \\ 0 & K_T \end{pmatrix}\begin{pmatrix} \cos\delta & -\sin\delta \\ \sin\delta & \cos\delta \end{pmatrix} \tag{2.154}$$

a) Horizontal dispersion coefficients

In the case of isotropic turbulence, the horizontal dispersion coefficient can be written as

$$K_H = A_2 \varepsilon^{2/3} \ell^{4/3} \qquad (2.155)$$

which is Richardson's well known "four-thirds power law", where ℓ is a characteristic lengthscale of the pollutant cloud, ε is the mean energy dissipation rate per unit mass, and A_2 is a non-dimensional constant. This equation is valid only when the diffusing eddies belong to the inertial subrange of the spectrum, i.e., the interval of the spectrum in which the eddies transfer all the energy they receive from bigger eddies to smaller eddies. In this situation, the only parameter controlling the energy is the energy dissipation rate, and equation (2.155) can be derived from dimensional analysis. However, Crickmore (1972) obtained diffusion rates in tidal coastal waters which were not compatible with Richardson's law, and he expressed his doubts about the convenience of applying (2.155) in these conditions; as an alternative, he proposed an equation for horizontal diffusion similar to that given earlier by Elder (1959) –see equation (2.160)-.

In the spectral band corresponding to energy input, the turbulent diffusivity becomes dependent on both the characteristic scale of turbulence and on numerous input conditions, so its estimation is not so easy. Moreover, if two input bands, corresponding to two different external energy sources, lay close to each other, and the inertial subrange of the lower band spectrum is occupied also by the energy input interval of the high band spectrum, it can be said that the diffusion coefficient will not obey the "four-thirds law". This could explain the fact that equation (2.155) has never been found to apply in coastal areas, where it is possible that two close frequency bands receive energy from two external sources of turbulence energy, namely waves and interactions between flowing water and the bottom morphology. However, the distance between both frequency bands may widen, making it possible for the relationship "4/3" to appear.

Additionally, in nearshore waters the power exponent is reduced because of the limits imposed by the boundary effects on the scales of the eddies available for mixing; Bowden (1983) has suggested that the exponent in coastal waters lies between 0.5 and 1.0. Figure 2.9, taken from Wood *et al.* (1993), shows the variation of the horizontal diffusivity (here ε_y) as a function of a characteristic patch lengthscale, assuming that the turbulence is isotropic. The dependency of K_H on the dissipation rate can be neglected when the problem of interest is very large, and equation (2.155) can be written as

$$K_H = A_1 \ell^{4/3} \qquad (2.156)$$

where A_1 is a constant which ranges from 0.002 to 0.01 $cm^{2/3}/s$ according to Okubo (1974), and from 0.0015 to 0.05 $cm^{2/3}/s$ following Koh and Brooks (1975).

In any case, the structure of the velocity field, *via* its gradients and spectral features, strongly influences the coastal dispersion (measured by the variance $\sigma^2$of a cloud of particles -$K_H \cong d\sigma^2/dt^2$-) and the apparent dispersion coefficient K_H (Zeidler, 1976). Another factor that shapes the variation of K_H is the distance to the shore: far off-shore turbulent eddies are allowed to develop freely before reaching a size comparable to that of the water body. When approaching the shore, they can only grow up to a lengthscale allowed by the local depth and the distance to the shoreline. Further, the size of the turbulent eddies may be restricted by the existence of a pycnocline, which impedes vertical diffusion.

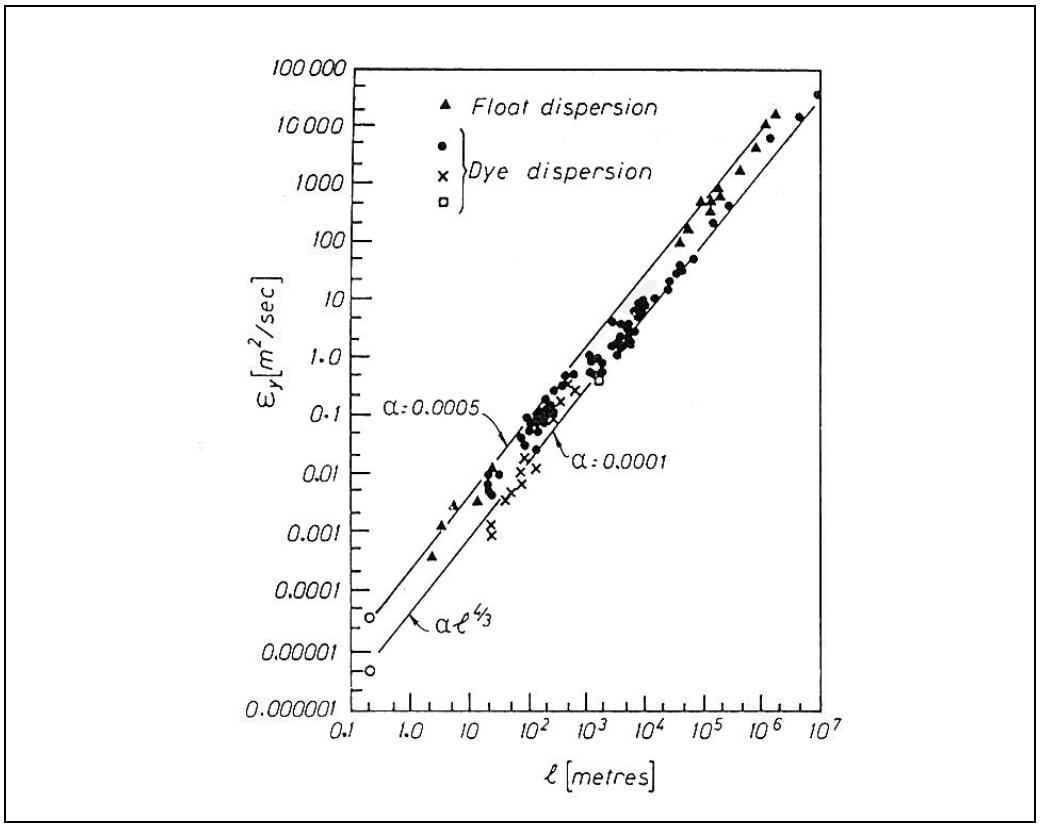

Figure 2.9: Horizontal diffusivity in the ocean as a function of a patch lengthscale (from Wood *et al.*, 1993).

The effects of velocity distribution and distance to the shore on dispersion coefficients can be seen in figures 2.10 and 2.11; the former shows the dependence of the exponent *n* in the relationship $\sigma^2 \sim t^n$ with the water velocity, whereas the latter shows its dependence with the relative distance to the shore (l_{min} and l_{max} are the size of the patch). It is clearly seen that the growth of the substance clouds decreases significantly when the distance to the shoreline becomes a few times greater than their lengths, while there seems to be a dramatic increase in the growth of dispersion when the ambient velocity increases beyond a given threshold. Zeidler (1976) points out that this phenomenon may be correlated with a critical Reynolds number for which turbulent eddies tend to enhance diffusion in the band of larger scales, that would possibly be coupled with higher velocities, but he remarks that definite conclusions should not be drawn from his data.

Several methods are available for calculating dispersion coefficients, but they all rely on assumptions such as a particular vertical velocity profile or a particular flow pattern. As an example, Fischer *et al.* (1979) investigated the longitudinal dispersion coefficient in a two dimensional laminar flow, and gave the following expression

$$K_L = -\frac{1}{hD_m}\int_0^h u' \int_0^y \int_0^y u' dy dy dy \qquad (2.157)$$

after assuming that a balance was established between the longitudinal advective transport and the cross-sectional diffusive transport, and that deviations of a variable (e.g., velocity, concentration) from its cross-sectional mean were small compared to the value of the mean. In fact, Gallagher & Hobbs (1978) point out that these assumptions are fundamental to the theoretical derivation of

dispersion coefficients, even though the first assumption is not valid when insufficient time has elapsed after the release for the equilibrium to be established ($t_{eq} \cong 0.4\ h^2/D_m$, Fischer *et al.*, 1979), and the second is invalid when high concentration gradients occur.

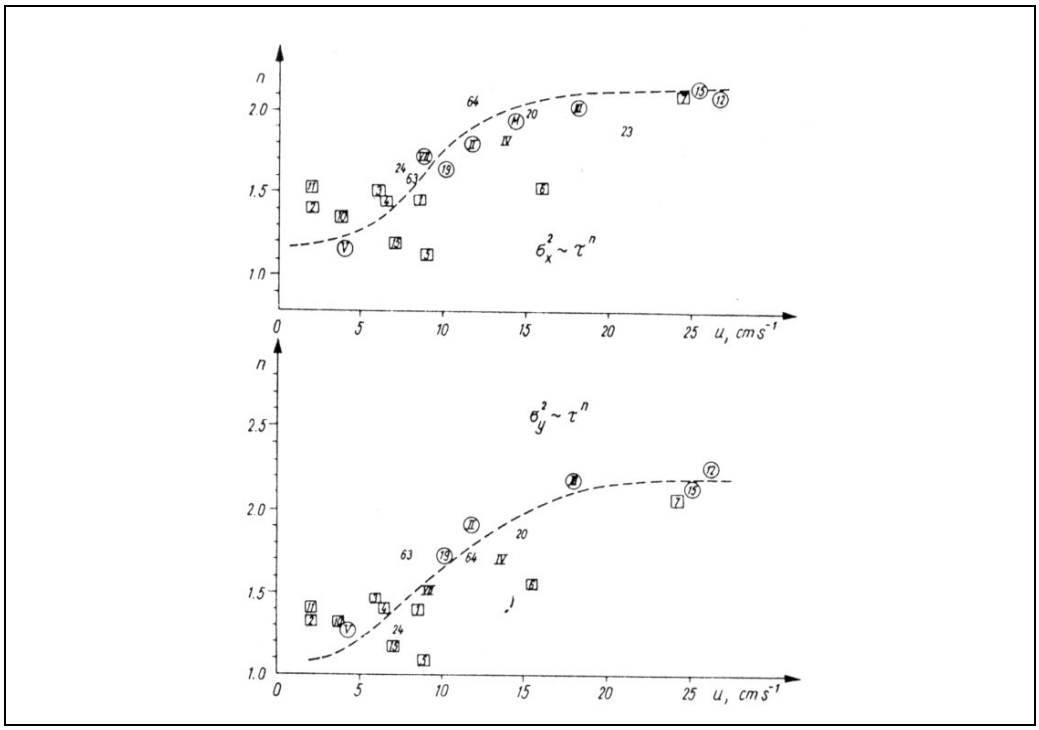

Figure 2.10: Effects of the velocity on the growth of dispersion (Zeidler, 1976).

The same authors (Fischer *et al.*, 1979) presented an equivalent expression for dispersion in turbulent flows, in which the cross-sectional (transverse) turbulent diffusion coefficient D_T was introduced to substitute the molecular diffusivity:

$$K_L = -\frac{1}{h}\int_0^h u' \int_0^y \frac{1}{D_T}\int_0^y u'\,dy\,dy\,dy \qquad (2.158)$$

and a generalisation of the dispersion coefficients for the case of flows in which velocity profiles exist in two directions (skewed shear flows, Fischer *et al.*,-1979-)

$$K_{i,j} = -\frac{1}{hD}\int_0^z u'_i \int_0^z \int_0^z u'_j\,dz\,dz\,dz \qquad (2.159)$$

The diagonal components K_{ii} and K_{jj} derived in equation (2.159) are equal to the ones that would be obtained if only velocity profiles in those directions (x_i and x_j) existed; the additional components K_{ij} and K_{ji} depend on the interaction of the x and y velocity profiles, and imply that a gradient in the x direction can produce a mass transport in the y direction, and viceversa.

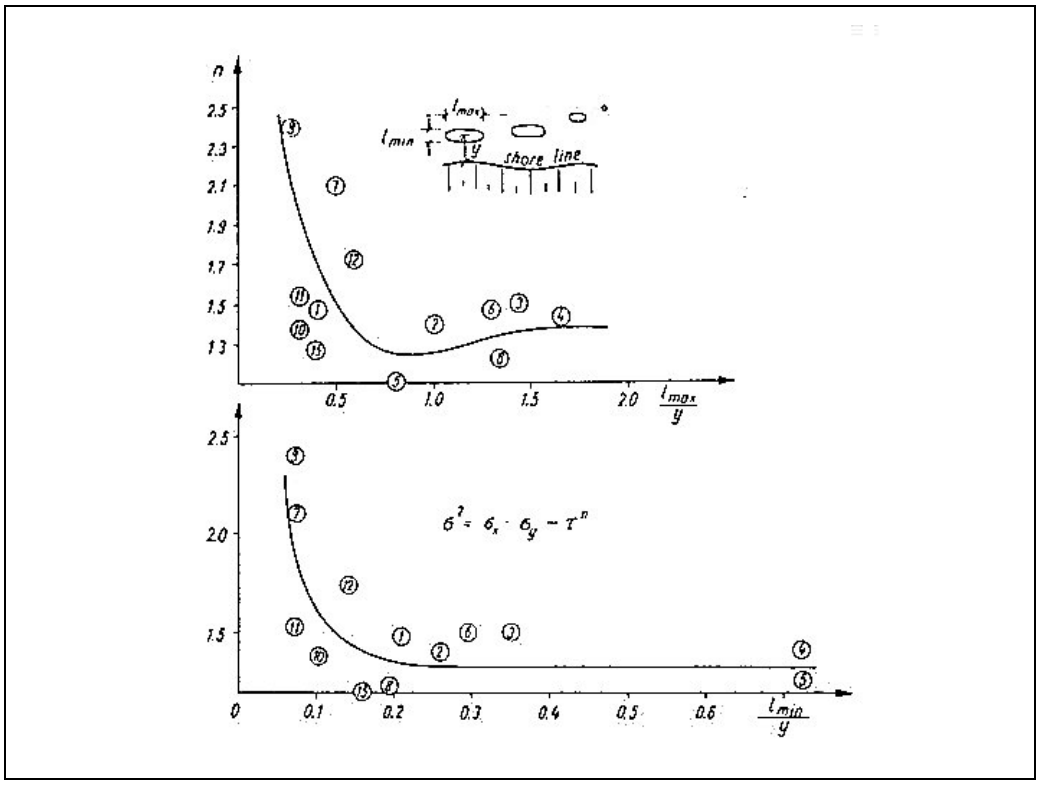

Figure 2.11: Effects of the distance to shore on the growth of dispersion (Zeidler, 1976).

Elder (1959) studied the dispersion of marked fluid in a 2DH flow and deduced expressions for the longitudinal and lateral dispersion coefficients as a function of the flow depth and the shear velocity at the bottom. His empirical coefficients are

$$\begin{aligned} K_L &= c_L h u_* \\ K_T &= c_T h u_* \end{aligned} \tag{2.160}$$

where the experimental constants are given by Elder as c_L = 5.9 and c_T = 0.23, assuming the velocity profile is logarithmic. Based on the work and concepts introduced by Elder (1959) and Taylor (1954), several authors have generalised the analysis of dispersion coefficients and found that, in irregular channels with arbitrary velocity profiles in the vertical direction, the longitudinal dispersion coefficient could be expressed as

$$K_{xy} = \alpha_B h u_* \tag{2.161}$$

where u_* is the shear velocity, h is the water depth, and α_B is a proportionality factor that lays in the range 6 to 200 and depends on the detailed form of the velocity profile. The lowest value corresponds approximately to Elder's (1959) "logarithmic profile" analysis, whereas the highest corresponds to a profile characteristic of the densimetric circulation in the saline reaches of an estuary. Crickmore (1972) mentions studies by Okoye (1970) in flumes in which he observed that α_B was a function of the depth/width aspect ratio of the flow section, so that $K_{xy} / u_* h$ increases with decreasing h / W.

Nadaoka *et al.* (1991), in their quasi-3D sediment transport model, assumed isotropic horizontal dispersion outside the surf zone, and considered coefficients in the form

$$K_x = K_y = 0.01 x_B \sqrt{h_B g} \qquad (2.162)$$

for their quasi-3D sediment transport model, where the subscript *B* refers to the values at the breaker line.

In the presence of non-steady flows, such as estuaries where the flow and ebb of the tides may be the predominant hydrodynamic features, the derivation of dispersion coefficients is somewhat different. Holley *et al.* (1970) distinguish between two regimes: in the first case, the time T_d required for the diffusion equilibrium to be established is small compared to the tidal period T_t, so that at each time the shear/diffusion balance perpendicular to the flow has time to adjust to the new values of the velocities, and no modification to the steady flow theory is required. In the second case, the diffusion perpendicular to the sheared flow will not have enough time to destroy the distortion of the concentration profile before it is removed by the reversal of the flow itself, and so the concentration distribution will remain undistorted. According to Holley *et al.* (1970), the longitudinal dispersion coefficient can be taken as

$$\begin{aligned} K_L(\text{tidal}) &= K_L(\text{steady flow}) && \frac{T_d}{T_t} > 0.1 \\ K_L(\text{tidal}) &= 10\left(\frac{T_d}{T_t}\right)^2 K_L(\text{steady flow}) && \frac{T_d}{T_t} < 0.1 \end{aligned} \qquad (2.163)$$

Measurements of dispersion coefficients in field or laboratory experiments show a large dependence on the dispersion direction with respect to the main flow direction, being the longitudinal coefficients much larger than those describing transverse dispersion. Ozmidov (1990), for instance, mentions experiments in the Baltic Sea that yield longitudinal coefficients in the range 0.042 to 2.68 m^2/s, whereas the transverse dispersion coefficients lay between 0.007 and 0.106 m^2/s.

b) Vertical dispersion coefficients

In contrast with the relative abundance of data for horizontal dispersion, there is a scarcity of data related to vertical dispersion. Koh and Brooks (1975) report values ranging from $4 \cdot 10^{-2}$ cm^2/s to 200 cm^2/s, generally inferred from temperature and salinity data. Values compiled by Ozmidov (1990) from experiments in different seas are found to be between $4 \cdot 10^{-2}$ and 35 cm^2/s. Other values for the vertical dispersion coefficients mentioned in Wood *et al.* (1993) are in the range 1 to 50 cm^2/s; according to the authors, the lower values appear to be typical of coastal waters where a degree of stratification exists, while the higher values relate to well-mixed conditions.

The vertical turbulent diffusion and, therefore, the vertical dispersion coefficients, must be significantly influenced by the density stratification of ocean waters. Several expressions have been given to correlate K_V with the density gradient ε_ρ, such as the one proposed by Koh and Brooks (1975):

$$K_V = -10^{-8} \frac{\rho}{\varepsilon_\rho} \qquad (10^{-6} < \varepsilon_\rho \rho < 10^{-2}\ m^{-1}) \qquad (2.164)$$

In the surface mixed layer, the vertical diffusion coefficient can be expected to depend on the wave characteristics, such as the wave height H_w and period T_w, as in the expression given in Koh and Brooks (1975):

$$K_V = 0.02 \frac{H_w}{T_w^2} \qquad (2.165)$$

Nadaoka *et al.* (1991) used an expression of the type (2.161) to include vertical dispersion in their transport model, with a value of 0.16 for α. Estimated values for this parameter range from 0.16 to 0.23.

2.3.1.3 Effects of non-breaking waves on pollutant dispersion

The estimate of pollutant concentrations is usually based upon a steady or quasi-steady state analysis. In a wave environment, however, the similarity of the turbulent eddy timescales and the typical wave periods may lead to a significant coupling between the turbulent fluctuations and the unsteadiness of the surrounding flow, thus invalidating the (quasi-) steady state approach to nearfield mixing models. Various researchers have highlighted the fact that pollutant discharges in wave environments differ significantly from those in steady or quasi-steady flows.

Several studies (Sharp, 1986; Chyan *et al*., 1991) have found that the oscillatory motion associated with the propagation of surface gravity waves has a considerable effect upon local mixing characteristics. In particular, the so-called "zone of flow establishment" (i.e., the region in which the velocity profile goes from the original top-hat distribution at the discharge location to a Gaussian distribution) is severely shortened, and a region of intense fluid mixing appears (Chyan and Hwung, 1994). In some circumstances, the transverse distribution of both the axial velocity and the substance concentration is no longer Gaussian. Furthermore, experiments done by some authors (e.g., Koole and Swan, 1994) show that the centreline velocity and concentration do not follow a typical exponential decay pattern, but rather a multi-stage decay due to three different wave-induced mixing mechanisms.

The observations of wave-induced plume motions suggest that the primary influence of the waves on the discharges is near the source, where the mean jet velocity and the wave-induced horizontal velocity are of the same order, and is due to the alternating direction of the oscillatory flow. So, during a wave cycle, the jet flow has the characteristics corresponding to a cross-current jet, a co-stream jet or a counter-stream jet, alternatively. When the wave-induced velocity opposes the jet velocity, the jet “explodes” and becomes plumelike significantly closer to the source than in a non-wave case; when the wave-induced velocity and the discharge velocity are in the same direction, the jet travels farther before becoming plumelike. The net result is a “spraying” effect at the source (fig. 2.12), which leads to an enlargement of the jet area in comparison with the turbulent pure jet, and to an enhancement of the jet dilution.

This periodic deflection of the jet trajectory has been observed in laboratory experiments using vertical (Chyan and Hwung, 1993) and horizontal jets (Chin, 1987). In the former situation, an additional opportunity for the high concentration fluid in the centre of the jet to mix directly with freshwater is provided by the so called “wave tractive mechanism”, in which large volumes of freshwater are attracted into the central region of the jet by wave motion, and then become trapped by the jet fluid above the deflection region during the following deflection.

Furthermore, near the origin of a vertical jet, slender streams of jet fluid are formed at the lee of the horizontal wave velocity. This phenomenon occurs only when the horizontal velocity of the wave motion predominates, and is closely related to the wake vortices induced by the interaction of the jet flow with the wave (Chyan and Hwung, 1993). Through the formation of wake vortices, the additional vertical vorticity induced by this interaction increases the dilution rate as well as the transverse scale of the jet flow. Although horizontal jets do not benefit from these improvements, the initial dilution rate of

an adequately oriented (i.e., orthogonal to the propagating wave) discharge is still more effective than a vertical one in a wave environment (Chyan and Hwung, 1993).

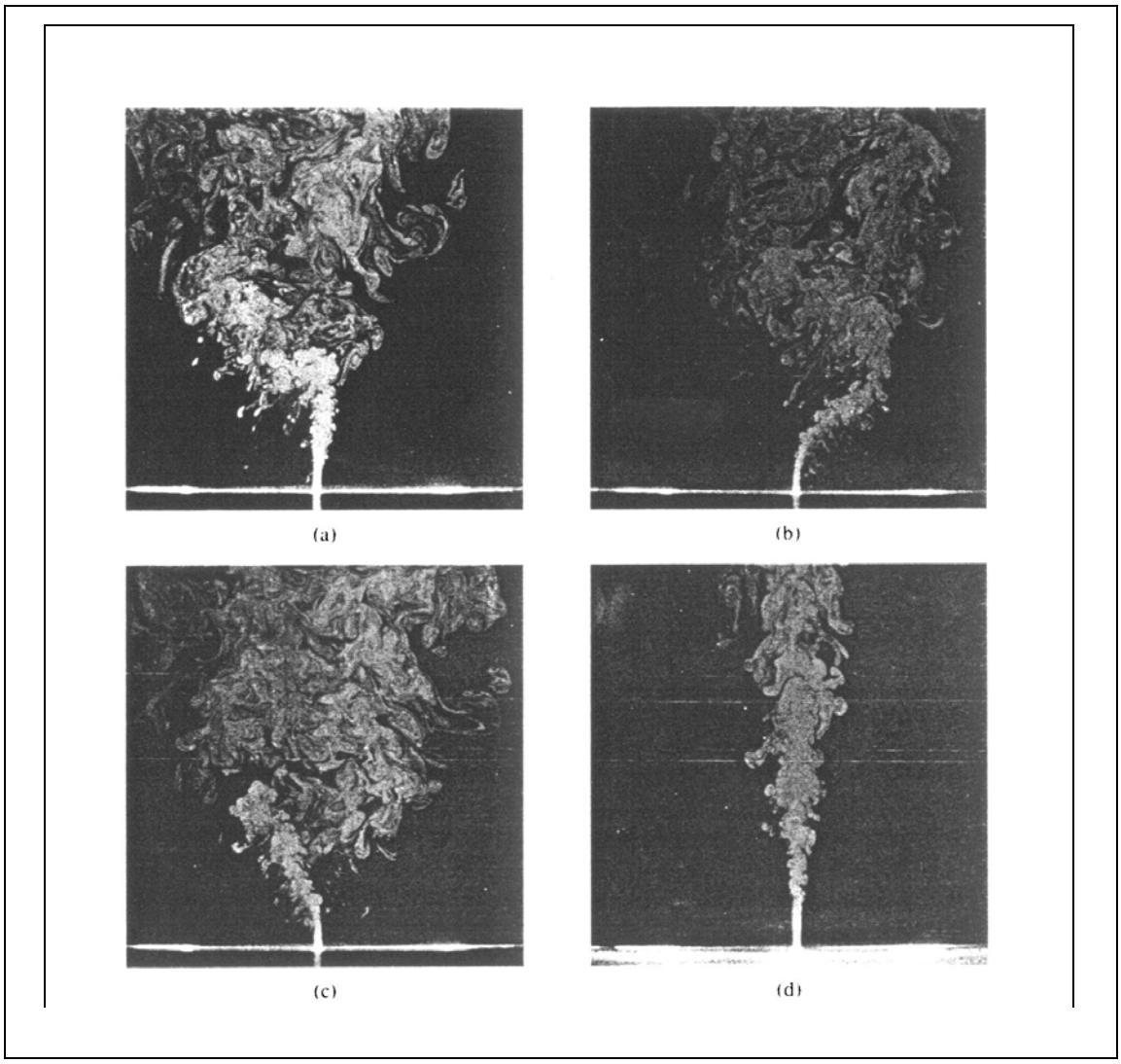

Figure 2.12: Longitudinal flow pattern of a pure jet (d) discharged into an oscillatory environment. Waves propagate from left to right, and the photographs are taken at t/T_w = 0.0 (a), 0.26 (b) and 0.67 (c). From Chyan and Hwung (1994).

Two common features appearing in numerous wave-dispersion experiments (e.g., Koole and Swan, 1994; Chyan and Hwung, 1993) are the occurrence of non-Gaussian velocity and concentration profiles, and an "anomalous" centreline decay. Some researchers have tried to explain the former effect by introducing an additional wave-induced mixing mechanism, but a simpler interpretation (Koole and Swan, 1994) suggests that these "flat-topped" or "bi-peaked" distributions result from the jet deflection due to periodic motion, and from the time-averaged analysis of the experimental data. The residence time of the jet at any spatial location within the region defined by the wave-induced displacement (l) increases with the distance from the jet axis, since the horizontal velocity is cyclic (figure 2.13); according to the magnitude of the ratio l/b, where b is the width of the jet, the maximum concentration will take place in

the centre ($l/b << 1$), on either sides ($l/b >> 1$) or in an extended central region ($l/b \approx 1$), reproducing a Gaussian, a "bi-peaked" or a "flat-topped" distribution, respectively, as shown in figure 2.14. This explanation is supported by the fact that the separation between peaks increases with the jet elevation, as corresponds to a larger water particle trajectory of wave motion (figure 2.15).

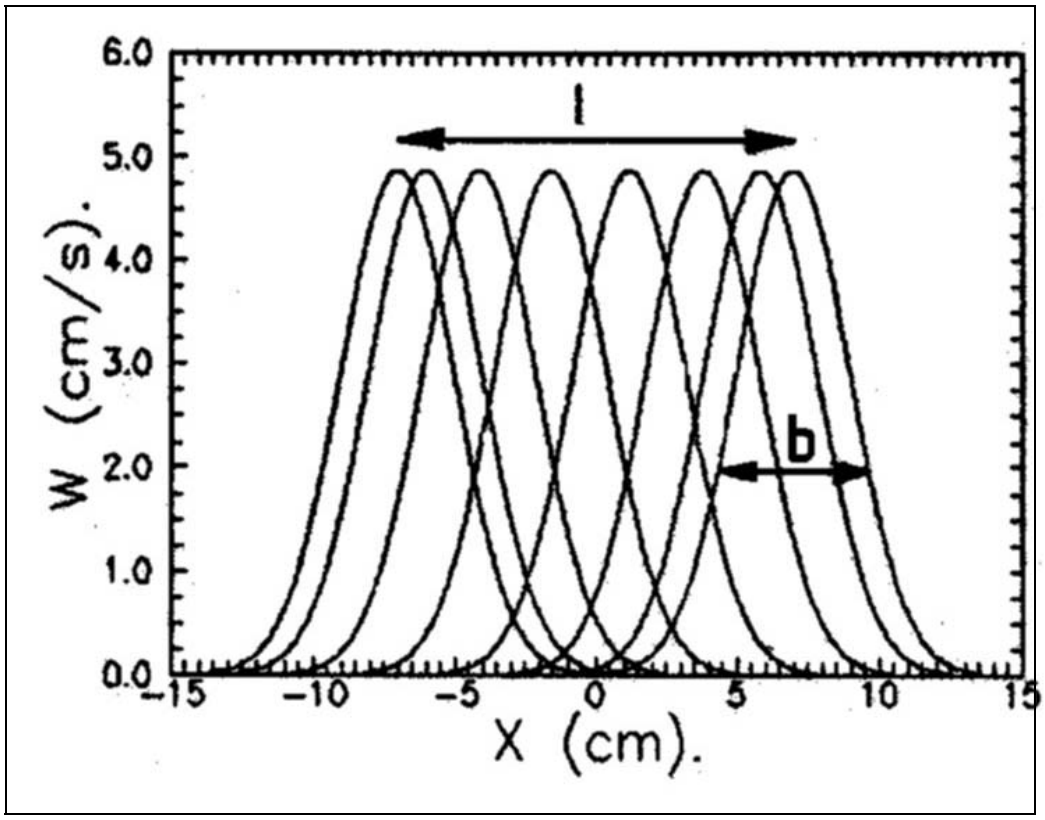

Figure 2.13: Lateral displacement of a Gaussian distribution (from Koole and Swan , 1994).

On the other hand, the decay of the time-averaged velocity and concentration along the axis, non-dimensionalised by their values at the source, presents a particular behaviour. The presence of wave motion transforms the exponential decay pattern seen in a quiescent environment into a multi-stage one (figure 2.16) where three distinct regions can be clearly defined: the "deflection region", closer to the source, characterised by a rapid dilution caused mainly by the jet wave-induced deflection; the "transition region", where the gradient can be positive, zero or negative depending on the wave strength (Chyan and Hwung, 1993); and the "developed region", where the gradient becomes less steeper since it corresponds to the developed jet area where wave influence is not too important. The apparent "un-mixing" of jet fluid in the transition zone can be explained by assuming a reduction of the wave-induced displacement of the jet axis at some height above the source, as can be seen in figure 2.17.

In addition to the wave-induced deflection, the oscillatory motion produces a significant increase in the rate at which ambient fluid is entrained into the emerging jet, not only due to the formation of wake vortices and the wave traction mechanism. The period of the oscillatory motion is typically close to the eddy timescales of the turbulent fluctuations, and there may be an important coupling between the turbulent fluctuations and the unsteadiness of the flow.

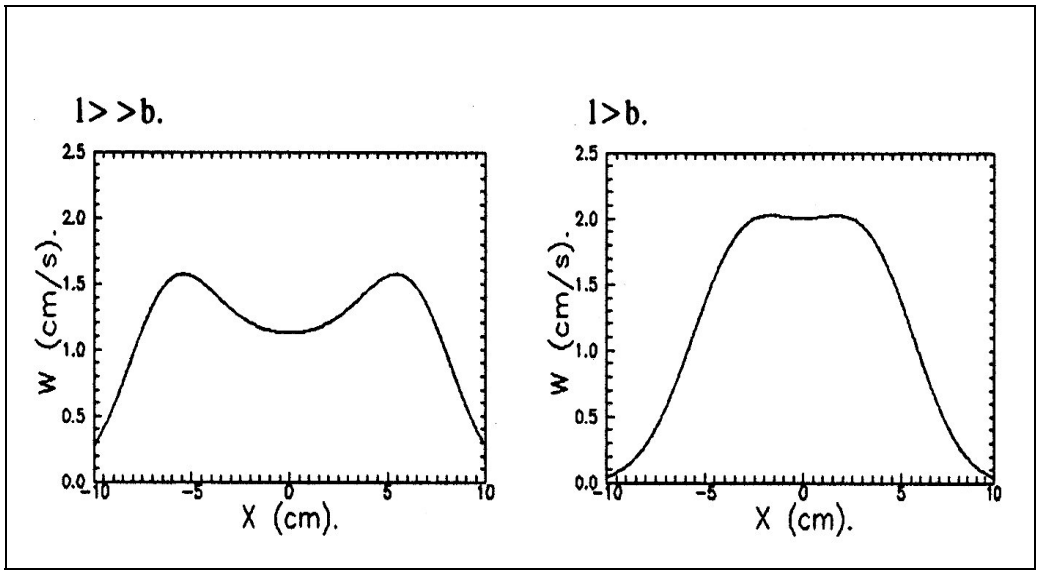

Figure 2.14: Time-averaged radial velocity distributions (from Koole and Swan , 1994).

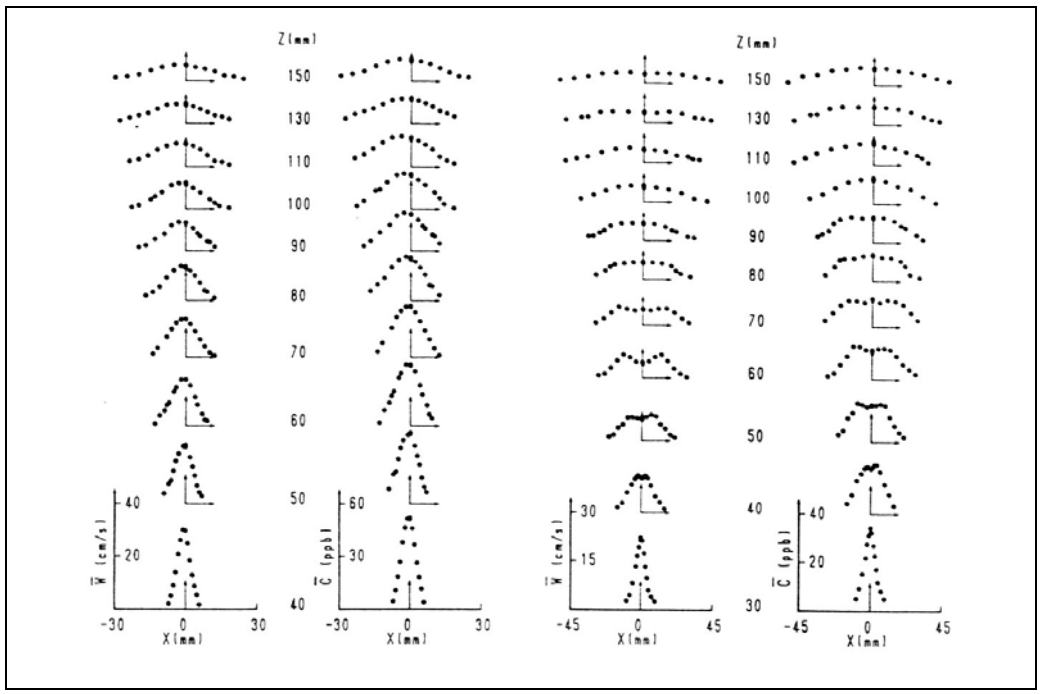

Figure 2.15: Cross-sectional profiles of mean velocity and concentration in a wave environment. a) T=0.52 sec., H_o/L_o=0.0508 ; b) T=0.85 sec., H_o/L_o=0.2251 (from Chyan and Hwung , 1994).

As found in experiments by Koole and Swan (1994), the wave motion encourages a transfer of energy into the turbulent components of the flow field, and the turbulent kinetic energy increases. The Reynolds shear stresses are substantially larger when the jet is discharged into a wave environment (figure 2.18); since these stresses represent the radial transport of axial momentum, this increase contributes to the rapid expansion of the jet, and its quick dilution.

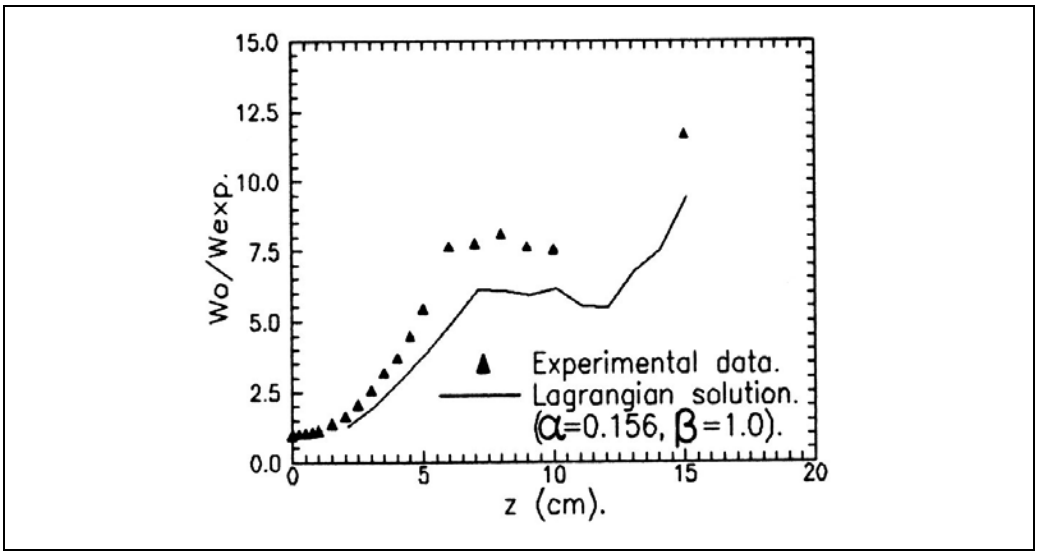

Figure 2.16: Decay of centreline velocity, according to Koole and Swan (1994). The coefficients α and β are the radial and forced entrainment coefficients, respectively, used in the Lagrangian solution.

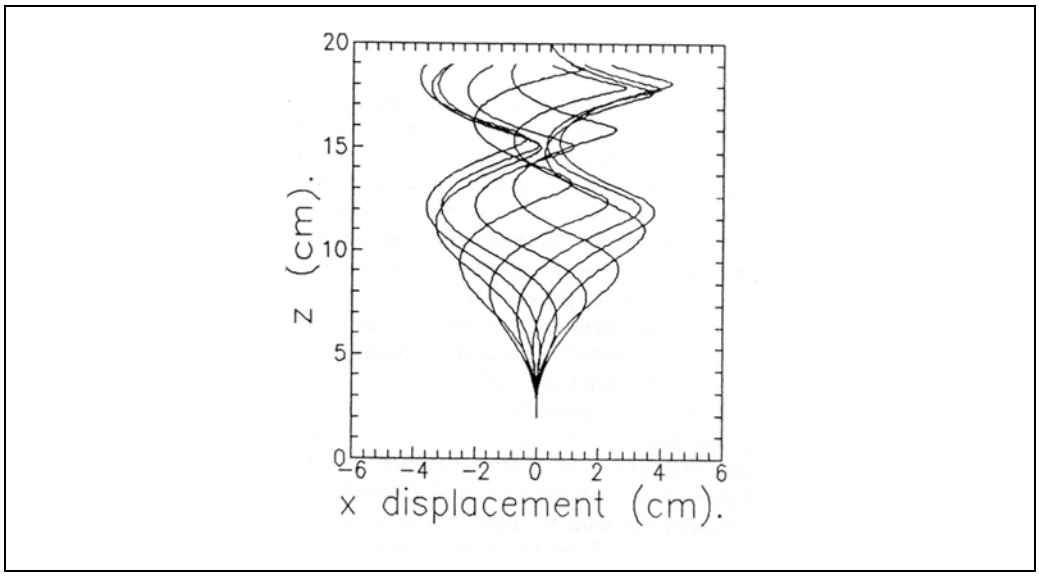

Figure 2.17: Trajectory of fluid elements in a wave environment (from Koole and Swan , 1994).

The transport and mixing induced by oscillatory motion significantly contribute to the dilution of discharged effluents. An accurate study of wave-induced mixing becomes necessary when analysing pollutant behaviour in coastal waters, because it may have a significant effect upon the concentration contours predicted in the far field.

Davydov's detailed work (1989) on the influence of surface waves on pollutant transport reveals that the effects of oscillatory motion on transport are twofold. First, they transfer the pollutants and, second, they enhance the turbulence level, thus stimulating the process of vertical mixing.

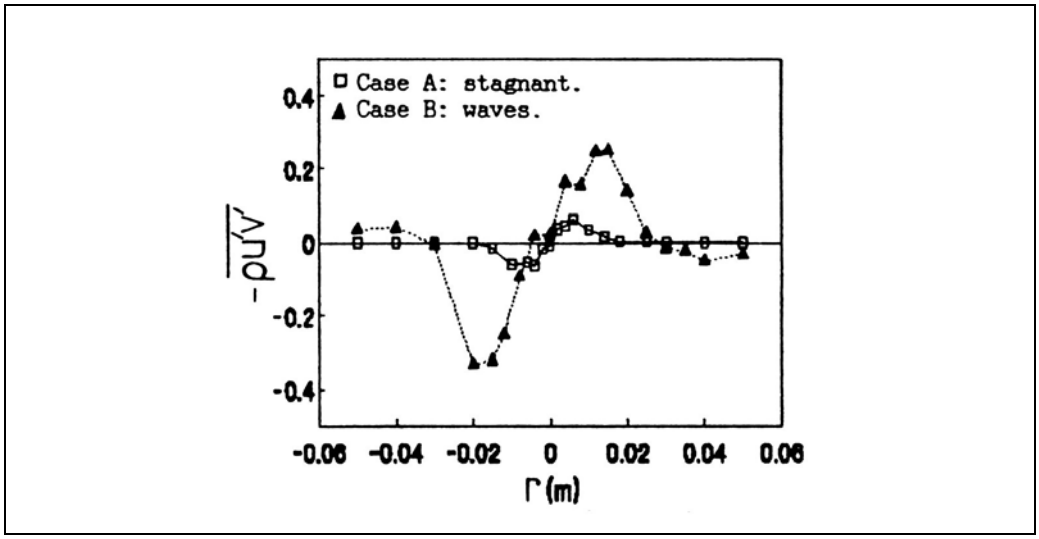

Figure 2.18: Reynolds shear stresses for stagnant and wave environment (from Koole and Swan , 1994).

a) Mass flow due to oscillatory motion

If a pollutant is discharged into a waterbody in which a wave field exists, it will move in the elliptical trajectory associated to water particles. Since the orbital trajectory is not a closed path, a slow motion in the direction of wave propagation will result. The total mass transport for small amplitude waves is obtained by integrating the mean vertical Lagrangian velocity times the fluid density, over the whole water column, i.e.,

$$M_x = \int_{-h}^{\eta} \rho \overline{u_L} dz = \frac{\rho g a_w^2 |\mathbf{k}|}{2\sigma} = \frac{E}{c_w} \tag{2.166}$$

Davydov (1989) substitutes the instantaneous values of velocity and concentration in the transport equation with the sum of mean values and wave-induced fluctuations (in a similar manner to equation 2.11) and, after time-averaging over a wave period, subtracts the resulting equation from the original transport equation. Neglecting members of order higher than the first with respect to wave slope $a_w|\boldsymbol{k}|$, he obtains (being $x_3=z$)

$$\frac{\partial c'}{\partial t} + u_i \frac{\partial c'}{\partial x_i} = -u'_i \frac{\partial C}{\partial x_i} + \frac{\partial}{\partial x_j}\left(K_H \frac{\partial c'}{\partial x_j} \right) + \frac{\partial}{\partial x_3}\left(K_V \frac{\partial c'}{\partial x_3} \right) \tag{2.167}$$

Neglecting small values of vertical velocity and diffusion, the solution to equation (2.167) is of the form

$$c'(t) = \frac{a_w}{\sinh\psi}\left(\cosh\varphi \frac{k_j}{|\mathbf{k}|} \frac{\partial C}{\partial x_j} \sin\chi - \sinh\varphi \frac{\partial C}{\partial x_j} \cos\chi \right) \tag{2.168}$$

where use has been made of the velocities for progressive waves as defined in linear theory:

$$u'_j = \frac{k_j}{|\mathbf{k}|}\alpha \cosh\varphi \cos\chi \qquad j = 1,2 \tag{2.169}$$

$$u'_3 = \alpha \sinh\varphi \sin\chi \tag{2.170}$$

$$\alpha = \frac{\sigma a_w}{\sinh\psi} \qquad \psi = |\mathbf{k}|h$$
$$\varphi = |\mathbf{k}|(h+z) \qquad n = \sigma + k_j u_j \tag{2.171}$$
$$\chi = k_j x_j - nt$$

Knowing the solutions for *u'* –eqs. (2.169) - (2.170)- and *c'* –eq. (2.168)-, the wave flow of pollutants q_j=-<$u'_i c'$> can be determined:

$$q_j = \delta_j \frac{\partial C}{\partial x_3} \qquad q_3 = -\delta_j \frac{\partial C}{\partial x_j}$$
$$\delta_j = \frac{\sigma a_w^2 \sinh 2\varphi}{4\sinh^2\psi}\frac{k_j}{|k|} \tag{2.172}$$

b) Turbulence enhancement due to oscillatory motion

The effects of wave flow on the horizontal dispersion coefficient K_H have been studied by Masch (1963), who correlated K_H with the surface current u_s and the resulting vector for orbital velocity u_{orb}. Basing his work on experimental data, he found that

$$K_H = 15.811 \cdot 10^{-3}(u_s + u_{orb})^{3.2} \tag{2.173}$$

or

$$K_H \cong \left(\frac{H_w}{L_w}\right)^2 \left(1 + \frac{2\pi H_w}{L_w}\right)\frac{H_w^2}{T_w} \tag{2.174}$$

for $u_s = 0$, where u_{orb} is, according to linear wave theory,

$$u_{orb} = \frac{\pi H_w}{T_w}\left\{\cos^2\left[2\pi\left(\frac{x}{L_w} - \frac{t}{T_w}\right)\right]\cosh\left(\frac{2\pi h}{L_w}\right) + \sin^2\left[2\pi\left(\frac{x}{L_w} - \frac{t}{T_w}\right)\right]\right\} \tag{2.175}$$

Zeidler (1976) used dimensional analysis to write a general expression for the dispersion coefficients

$$K \propto a_w^2 T_w^{-1} f\left(a_w L_w^{-1}, L_w^2 T_w^{-1} \nu^{-1}, z L_w^{-1}, g h L_w^{-2} T_w^{\,2}\right) \tag{2.176}$$

where *f* is an unknown function. Based on data from experiments in a wave flume, he obtained an estimation for the coefficients as a function of a "Reynolds number" Re_w:

$$K_L = 1.8 \cdot 10^{-6} \, Re_w^{2.4} \tag{2.177}$$

$$K_T = 8.0 \cdot 10^{-5} \, Re_w^{1.7} \tag{2.178}$$

$$Re_w = \frac{a_w^2}{\nu T_w}\left[\sinh\left(\frac{2\pi h}{L_w}\right)\right]^{-1/4} \tag{2.179}$$

The fitting between equation (2.177) and (2.178) and experimental data is shown in figure 2.19. Here, the longitudinal coefficient ($K_L \equiv K_{wx}$) is parallel to the wave ray, and the lateral coefficient ($K_T \equiv K_{wy}$) is parallel to the wave crest.

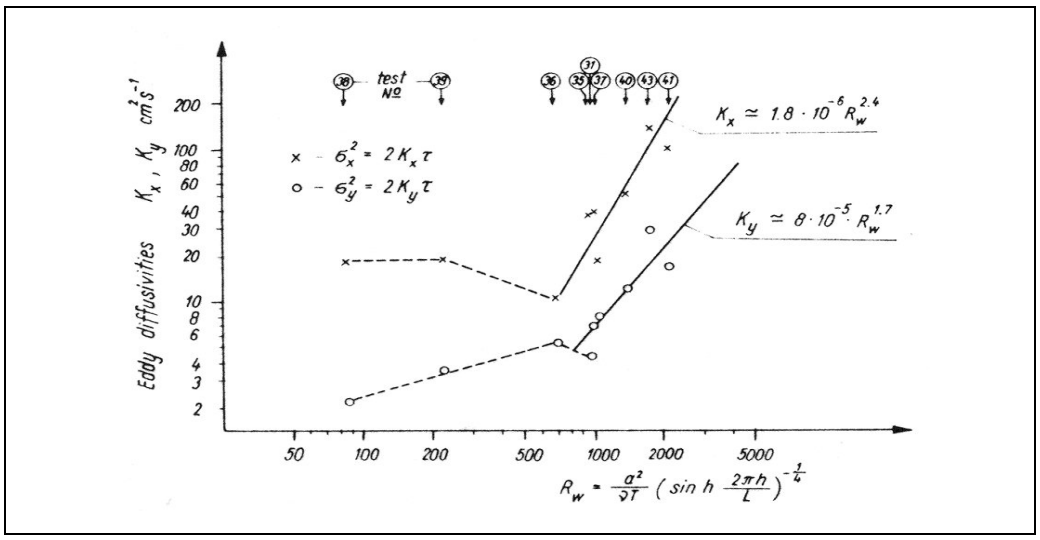

Figure 2.19: Eddy diffusivities due to oscillatory motion (from Zeidler, 1976).

A different approach was followed by Davydov (1989) for the vertical dispersion. He used a simplified two-equation turbulence model,

$$\frac{\partial k}{\partial t} = \frac{\partial}{\partial z}\left(K\frac{\partial k}{\partial z}\right) + P - \varepsilon \tag{2.180}$$

$$\frac{\partial \varepsilon}{\partial t} = \frac{\partial}{\partial z}\left(K_\varepsilon \frac{\partial \varepsilon}{\partial z}\right) + \frac{\varepsilon}{k}\left(c_1 P - c_2 \varepsilon\right) \tag{2.181}$$

$$P = K^*\left[\left(\frac{\partial u_j}{\partial z}\right)\left(\frac{\partial u_j}{\partial z}\right) + \alpha_r g \frac{\partial \rho}{\partial z}\right] \tag{2.182}$$

with

$$K^* = \alpha\frac{k^2}{\varepsilon}; \quad K = K^* + \nu; \quad K_\varepsilon = \alpha_\varepsilon K^* \tag{2.183}$$

and where c_1, c_2, α_ε, α_r, and α are constants which depend on the particular type of flow, P is the rate of generation of turbulent energy, and K^*, K, and ν are coefficients of turbulent, total and kinematic viscosity.

Davydov (1989) defined the energy generation term as the combination of a part due to production by a vertical shift in the horizontal velocity component, one due to density stratification, and a third due to vertical shifts in the horizontal component of wave velocity u'_j:

$$P = K^*\left[P_C + P_B + \alpha_r g\frac{\partial \rho}{\partial z}\right] \tag{2.184}$$

$$P_C = \frac{\partial u_j}{\partial z}\frac{\partial u_j}{\partial z} \quad ; \quad P_B = \left\langle \frac{\partial u'_j}{\partial z}\frac{\partial u'_j}{\partial z} \right\rangle \tag{2.185 a, b}$$

where the brackets denote wave-period averaging. After substituting equation (2.169) in (2.185 b), the wave-generated production term can be written as:

$$P_B = \frac{1}{2}\left(\frac{\sigma a_w |\mathbf{k}| \sinh\varphi}{\sinh\psi}\right)^2 \tag{2.186}$$

2.3.1.4 Effects of breaking waves on pollutant dispersion

As a wave approximating the shoreline breaks, the overturning wave front curls forward, forming a jet that impacts on the surface ahead and creating a cavity full of air which rapidly collapses. The air mixes with the water in a region with vortical motion and of a high concentration of bubbles.

The impact of the jet farther down on the wave surface causes a wedge-shaped amount of water to splash up, curl, and form a secondary jet that impacts on the water below it, and so on several times. The result is a series of two-dimensional vortex-like coherent structures, with axes roughly parallel to the wave crest, and with large shear rate in the intermediate regions (Battjes, 1988).

The two-dimensional horizontal vortices break down (Nadaoka and Hirose, 1986) into smaller vortices that originate in the areas of maximum strain between horizontal eddies, and extend obliquely downward. Dye experiments in this region show (Nadaoka and Hirose, 1986) that the horizontal eddies play an important role in cross-shore dispersion, whereas the oblique vortices transport the dye to the bottom of the water column.

Finally, the large-scale water motions degenerate into small-scale motions, increasingly disordered, which can eventually be considered as turbulence when coherent structures can no longer be identified.

This increase in local turbulence levels leads to a significantly large growth in mixing rates, which has to be accounted for by the dispersion coefficients.

a) Mass flow

According to Stive and DeVriend (1987), the mass flow generated by wave breaking can be estimated as

$$M_B = \left(1 + \frac{7h_B}{L_{wB}}\right)\frac{E_B}{c_w} \tag{2.187}$$

with E_B equal to the energy density of the breaking wave field. Since this mass flow occurs above the wave trough level, it contributes mainly to the advection of buoyant substances.

b) Dispersion coefficients

Inside the surf zone, the turbulent diffusion coefficient is generally assumed to be horizontally isotropic. In their sediment transport model, Nadaoka *et al.* (1991) did precisely this and, following Longuet-Higgins (1970), used a diffusivity similar to that of equation (2.162), but variable across the surf zone:

$$K_H = 0.01 x_B \sqrt{gh} \tag{2.188}$$

where x_B is the cross-shore distance.

A different formulation for horizontal diffusivity was given by Thornton (1970) who, after assuming stationary conditions and a slowly sloping bottom, and comparing laboratory data with field measurements, obtained the following expression for the diffusivity:

$$K_H = \frac{H_w^2}{8\pi^2}\frac{gT_w}{h}\cos^2\alpha_w \tag{2.189}$$

where α_w is the incidence angle of the wave field. De Vriend and Stive (1987) estimated the turbulent diffusivity as

$$K_H = K_{wc} + K_B \tag{2.190}$$

where K_{wc} is the coefficient describing the mixing due to wave and current effects, and K_B characterises the mixing due to breaking induced turbulence:

$$K_{wc} = c_{VS}\kappa h w_* \quad \text{(de Vriend and Stive, 1987)} \tag{2.191}$$

$$K_B = c_2 h\left(\frac{D_B}{\rho}\right)^{1/3} \quad \text{(Battjes, 1975)} \tag{2.192}$$

with κ equal to the von Karman constant (κ=0.41) and w_* equal to the wave-current shear velocity, and where D_B is the rate of wave energy dissipation per unit area, due to breaking, and both c_{VS} and c_2 are "constants" that depend strongly on whether the mixing is vertical or horizontal. The wave energy dissipation rate can be calculated as (Battjes and Jansen, 1978):

$$D_B = \frac{\alpha_{BJ}}{4} g\rho H_{wM}^2 f_p Q_B \tag{2.193}$$

$$\frac{1 - Q_B}{\log Q_B} = \left(\frac{H_{w,rms}}{H_{wM}}\right)^2 \tag{2.194}$$

where Q_b is the fraction of broken waves, f_p is the peak frequency, $H_{w,rms}$ is the root-mean-square wave height, H_{wM} is the depth-limited wave height -equation (2.57)-, and α_{BJ} is a constant expected to be of order one.

Another expression for K_H has been proposed by Battjes (1983) and Svendsen (1987) as

$$K_H = l\left(\frac{\beta}{c_d}\frac{l}{h}\right)^{1/3}\left(\frac{D_B}{\rho}\right)^{1/3} \tag{2.195}$$

with l a turbulent length scale proportional to the water depth ($l=\alpha_S h$), and α_S and c_d constants. Svendsen (1987) expected α_S to be between 0.2 and 0.3, while Rodriguez *et al.* (1995) found experimental values for α_S between 0.2 and 0.5, depending on the measuring position across the surf zone. Using the values α_S =0.3, β=1, and c_d = 0.09, and comparing eqs. (2.192) and (2.195), a value for the parameter c_2 can be determined, being c_2 = 0.45.

Inside the surf zone, Nadaoka and Hirose (1986) derived an expression for the vertical diffusivity involving the bottom slope i and the wave length L:

$$K_V = 0.18\gamma_w^{7/3} L_w^{1/3} h^{2/3} (gh)^{1/2} i^{1/3} \tag{2.196}$$

where $\gamma_w = H/h$ = 0.8.

2.4 CONCLUSIONS

The hydrodynamics of coastal and estuarine regions present certain characteristics that differentiate them from general open sea hydrodynamics, the most evident being the breaking of waves and the generation of coastal currents due to the presence of a solid boundary.

A very important role in coastal hydrodynamics is played by the wind, since it contributes to both the steady and the oscillatory component of water motion. In the first case, the wind drag on the water surface induces vertically-varying currents that may extend over the whole watercolumn in shallow waters; in the second case, the action of the wind generates the most frequent, and most important, of all the surface waves. Wind-induced currents may be described using a series of different formulations, depending on the assumptions introduced; similarly, wind-waves are also explained by several theories, the most simple (and most extended) of which is the linear theory, based on a “small amplitude” assumption. The solid boundaries and the decrease in waterdepth that define a coastal region are also important agents in characterising the hydrodynamic field; they help induce wave-breaking, wave field refraction and diffraction, longshore currents, undertow, and rip currents, amongst others. In addition, tidal currents and estuarine circulation must also be considered in coastal hydrodynamics.

As is obvious, these particular features of water dynamics are reflected in the transport and dispersion of pollutants and natural substances (e.g., nutrients), either directly in the form of a bulk transport (water currents, waves), or through the increase and decrease of the level of marine turbulence, as is the case of wave breaking in the surf-zone, wave-induced turbulence further offshore, or turbulent enhancement at the salt wedge interface in estuaries.